Commission of the European Community

JOINT
RESEARCH
CENTRE

NEANDC (E) 232 "U" Vol. III Euratom

INDC (EUR) 016/G

ANNUAL PROGRESS REPORT ON NUCLEAR DATA 1981

CENTRAL BUREAU FOR NUCLEAR MEASUREMENTS

GEEL (BELGIUM)

March 1982

Commission of the European Community

JOINT
RESEARCH
CENTRE

NEANDC (E) 232 "U" Vol. III Euratom
INDC (EUR) 016/G

ANNUAL PROGRESS REPORT ON NUCLEAR DATA
1981

CENTRAL BUREAU FOR NUCLEAR MEASUREMENTS

GEEL (BELGIUM)

March 1982

TABLE OF CONTENTS

NUCLEAR DATA

1. NEUTRON DATA

1.1 CROSS SECTIONS OF ACTINIDES

Fission Cross-section of ^{233}U and ^{241}Pu

C. Wagemans*, A. Deruytter, R. Barthélémy, J. Van Gils**

A 4ns time-coder with a microprocessor based accordeon system has been coupled to the 16.384 channels Tridac (Intertechnique) analyser. The result is an improved time-of-flight resolution and a considerably larger dynamic range than available before. With this improved equipment, a test run was done at a 9.3 m flight-path. We demonstrated that with a 100 Hz repetition frequency of GELINA, the neutron energy region from 10^{-2} eV up to 10^{5} eV can be covered in one single fission cross section measurement. In this way a step-wise normalization of the data can be avoided which results in an increased accuracy. Back-to-back ^{233}U and ^{10}B-layers viewed by surface barrier detectors were used and so the $^{233}U(n,f)$-fragments and the $^{10}B(n,\alpha)$-particles were detected simultaneously in the same position in the neutron beam. Each spectrum was stored in 8192 channels of the Tridac. This test measurement clearly illustrated the feasibility of the approach.
Fig. 1.1 shows the (moderated) neutron flux distribution in function of the neutron energy deduced from the present $^{10}B(n,\alpha)$ time-of-flight spectrum. Further measurements are needed to reach a sufficient statistical accuracy.
With the same set-up, the $^{241}Pu(n,f)$ cross-section was measured from 0.01 eV up to 30 keV. Also here, further measurements are needed to reach a sufficient statistical accuracy. In Fig. 1.2 a partial result is shown for $\sigma_f(E)\sqrt{E}$ for ^{241}Pu in the neutron energy region from 0.01 to 1 eV.

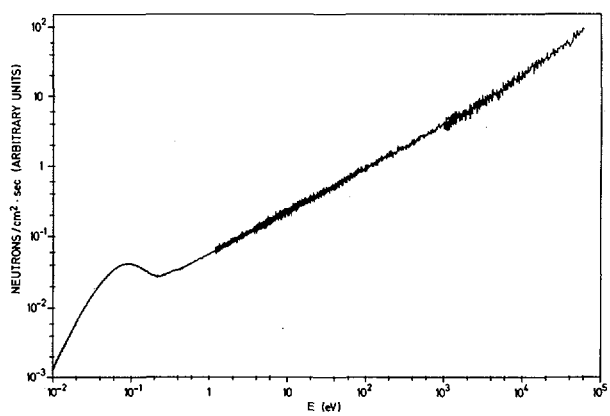

Figure 1.1 Neutron flux deduced from $^{10}B(n,\alpha)$ spectrum.

* SCK/CEN, Mol and R.U. Gent, Belgium
** SCK/CEN, Mol, Belgium

Fission fragment mass- and energy distributions for the neutron induced fission of ^{235}U and ^{241}Pu as a function of the spin of the resonances

E. Allaert*, C. Wagemans*,
G. Wegener-Penning**,
A. Deruytter, R. Barthélémy

The measurements of the $^{235}U(n,f)$-fragment mass- and energy-distributions have been analysed. The results will be compared with other fission characteristics in the resonance region and interpreted. Similar measurements are in execution for the $^{241}Pu(n,f)$ resonances.

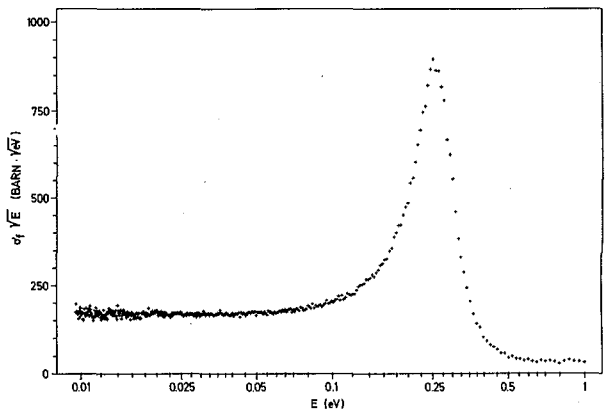

Figure 1.2 ^{241}Pu fission cross section.

Fission fragment mass- and energy distributions for the thermal neutron induced fission of ^{241}Pu and the spontaneous fission of ^{242}Pu

E. Allaert*, C. Wagemans*,
G. Wegener-Penning**,
A. Deruytter, R. Barthélémy

The measurements have been completed. The analysis reveals several striking differences between the spontaneous fission of ^{242}Pu and the thermal neutron induced fission of ^{241}Pu. As can be seen in Fig. 1.3, the $^{242}Pu(s,f)$ mass-distribution is much narrower and the peak yield is much higher than for the neutron induced fission. Also the total fragment kinetic energy (E_{tot}) distributions behave different (Fig. 1.4):

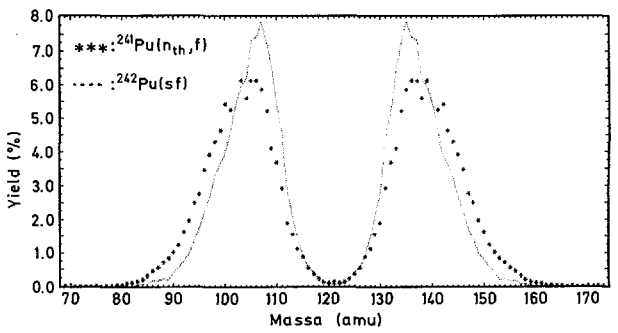

Figure 1.3 Fission fragment mass-distribution for $^{241}Pu(n_{th},f)$ and $^{242}Pu(sf)$.

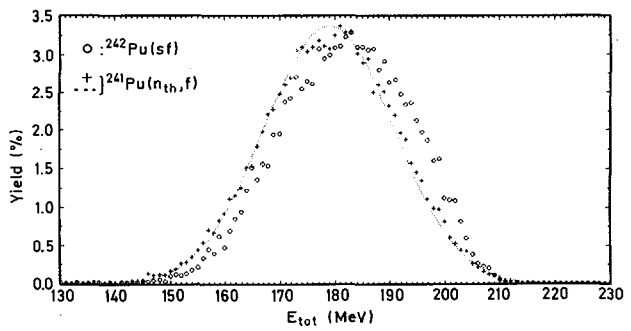

Figure 1.4 Total fragment kinetic energy distribution for $^{241}Pu(n_{th},f)$ and $^{242}Pu(sf)$.

---

* SCK/CEN, Mol and R.U. Gent, Belgium
** SCK/CEN, Mol, Belgium

for $^{241}Pu(n_{th},f)$ the E_{tot}-values are compatible with a Gaussian distribution (intermittent line), while in the spontaneous fission case the distribution is somewhat asymmetric. A more striking observation is the fact that $\bar{E}_{tot}$ is about 3 MeV higher for $^{240}Pu(s,f)$ despite the fact that its excitation energy is 6.3 MeV lower than for $^{241}Pu(n_{th},f)$. Finally, the mass-energy correlations clearly demonstrate the presence of shell effects. All these results are being interpreted now in the frame of the scission point model of Wilkins et al. (1). For comparison purposes, a similar measurement is in preparation for the spontaneous fission of ^{244}Pu, for which no literature data are available.

Measurement of the neutron induced fission and capture cross sections, and alpha of ^{235}U in the keV region

F. Corvi, L. Calabretta★, M. Merla, M.S. Moore★★, T. van der Veen

Average values

The analysis of the data averaged over given energy intervals is nearly completed. The values of $\bar{\sigma}_f$, $\bar{\sigma}_\gamma$ and $\alpha = \bar{\sigma}_\gamma/\bar{\sigma}_f$, deduced from the present measurement, are listed in Table 1.1 for the energy range from 2 to 85 keV. The errors quoted for $\bar{\sigma}_f$ go from 1 % at 1 keV to 3 % at 100 keV with logaritmic interpolation in between: they represent an estimate of the uncertainty in the shape of the neutron flux, measured with a thin ^6Li glass. The errors listed for α are inclusive of the uncertainty in the background subtraction and in the fraction of undetected fissions. The last one was calculated assuming that the fission chamber efficiency is known to 1 % precision. Finally, the relative errors on $\bar{\sigma}_\gamma$ are obtained by combining quadratically those of $\bar{\sigma}_f$ and α. To those errors one should add the uncertainty in the normalization procedure which is estimated about 1 % for $\bar{\sigma}_f$ and 4 % for α and $\bar{\sigma}_\gamma$.

---

(1) Wilkins et al.
Phys. Rev. 14, 1832 (1976)

★ Bursary of the European Community

★★ Visiting scientist from LASL

Table 1.1

^{235}U average neutron cross sections

Energy interval (keV)	$\bar{\sigma}_f$ (b)	$\bar{\sigma}_\gamma$ (b)	$a = \bar{\sigma}_\gamma/\bar{\sigma}_f$
2.0 - 3.0	5.231 ± 0.073	1.898 ± 0.23	0.363 ± 0.045
3.0 - 4.0	4.684 ± 0.072	1.615 ± 0.16	0.345 ± 0.035
4.0 - 5.0	4.157 ± 0.069	1.435 ± 0.13	0.345 ± 0.031
5.0 - 5.8	3.772 ± 0.065	1.166 ± 0.12	0.309 ± 0.033
6.0 - 7.0	3.235 ± 0.059	1.234 ± 0.12	0.381 ± 0.036
7.0 - 8.0	3.148 ± 0.059	1.171 ± 0.09	0.372 ± 0.028
8.0 - 9.0	2.937 ± 0.057	1.296 ± 0.08	0.441 ± 0.026
9.0 - 10	3.080 ± 0.061	1.111 ± 0.070	0.361 ± 0.022
10 - 12	2.645 ± 0.054	0.967 ± 0.060	0.366 ± 0.021
12 - 14	2.581 ± 0.055	0.926 ± 0.054	0.359 ± 0.020
14 - 16	2.451 ± 0.053	0.846 ± 0.049	0.345 ± 0.018
16 - 18	2.297 ± 0.051	0.883 ± 0.045	0.384 ± 0.018
18 - 20	2.325 ± 0.053	0.745 ± 0.041	0.321 ± 0.016
20 - 25	2.148 ± 0.050	0.770 ± 0.038	0.359 ± 0.016
25 - 30	2.060 ± 0.050	0.683 ± 0.035	0.332 ± 0.015
30 - 33	2.016 ± 0.050	0.630 ± 0.045	0.312 ± 0.021
38 - 40	1.870 ± 0.049	0.561 ± 0.049	0.300 ± 0.025
40 - 50	1.835 ± 0.049	0.572 ± 0.042	0.312 ± 0.021
50 - 60	1.781 ± 0.049	0.537 ± 0.036	0.301 ± 0.018
60 - 70	1.727 ± 0.049	0.523 ± 0.034	0.302 ± 0.018
70 - 80	1.652 ± 0.048	0.482 ± 0.038	0.291 ± 0.021
80 - 85	1.580 ± 0.046	0.468 ± 0.048	0.297 ± 0.029

In Fig. 1.5 the present cross section values are compared to those previously known, namely the ENDF/B-V values for $\bar{\sigma}_f$ and the values of Gwin et al.[1] for $\bar{\sigma}_\gamma$. A remarkably good agreement is noted between the two sets of $\bar{\sigma}_f$ values over the whole energy range, our data

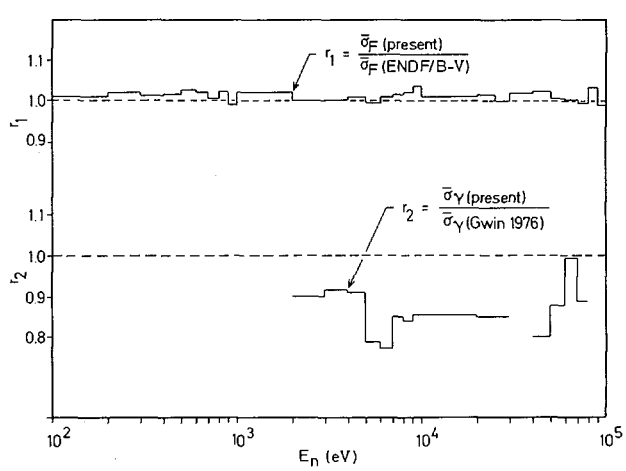

Figure 1.5 Fission cross section of ^{235}U. Comparison of present results with previously known values.

(1) R. Gwin et al. Nucl. Sci. Eng. 59, 79 (1976)

being, on the average, only 1.2 % larger than the ENDF/B-V points. On the contrary, there is a considerable disagreement for $\bar{\sigma}_\gamma$; on the average our data are 14 % lower than those of Gwin et al. Such a discrepancy both for its magnitude and its systematic character can only be due to an error in the normalization of one of the two measurements.

Fluctuation Analysis

Intermediate structure in the neutron induced fission cross section of ^{235}U below 50 keV is by now well established (1). In order to investigate further this matter, M.S. Moore will carry out an analysis of our fission and capture data in the range 2-30 keV to obtain average parameters for a width correlation study.

Alpha in the resonance region

Capture and fission "yield" data have been produced in the range 6-140 eV. These data do not represent cross sections but they are so normalized that their ratio for a given channel yields directly alpha. An example of such data in the range 6-29 eV is given in Fig. 1.6.
This information on alpha will be used by M.S. Moore for his evaluation of ^{235}U resonance parameters up to 100 eV.

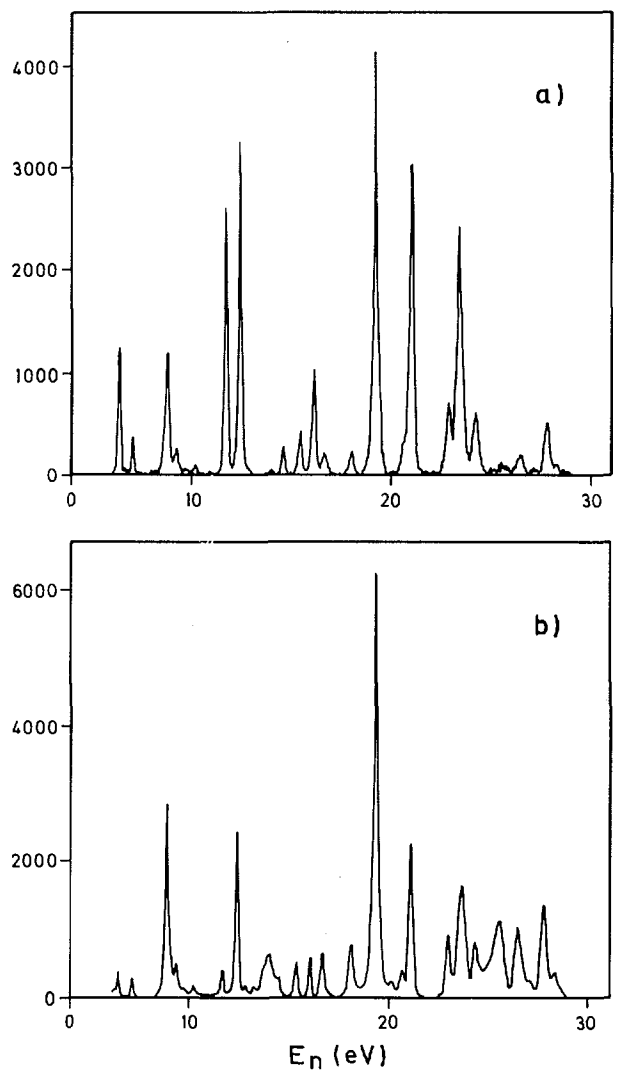

Figure 1.6 ^{235}U: a) capture "yield"
b) fission "yield".

(1) M.S. Moore et al.
Phys. Rev. C18, 1328 (1978)

Fission cross section of ^{238}Pu

H.-H. Knitter, C. Budtz-Jørgensen, D.L. Smith*, R. Vogt

The evaluation of the ^{238}Pu fission cross section from the raw experimental data obtained by the measurements at the Van de Graaff accelerator was completed. This data set, shown in Fig. 1.7 consists of about 80 fission cross section points distributed over the incident neutron energy range from 150 keV to 10 MeV. Below about 4 MeV, comparison can be made with already existing data, whereas in the range from 4 to 10 MeV the present data form the only existing set. From the first- and second-chance fission thresholds, estimates for the heights of the inner barriers of ^{239}Pu and ^{238}Pu were made. These estimates yielded the values of $V_A^9 = (6.14 \pm 0.15)$ MeV and $V_A^8 = (5.77 \pm 0.20)$ MeV. An internal report describes these measurements at the Van de Graaff accelerator and gives the results.

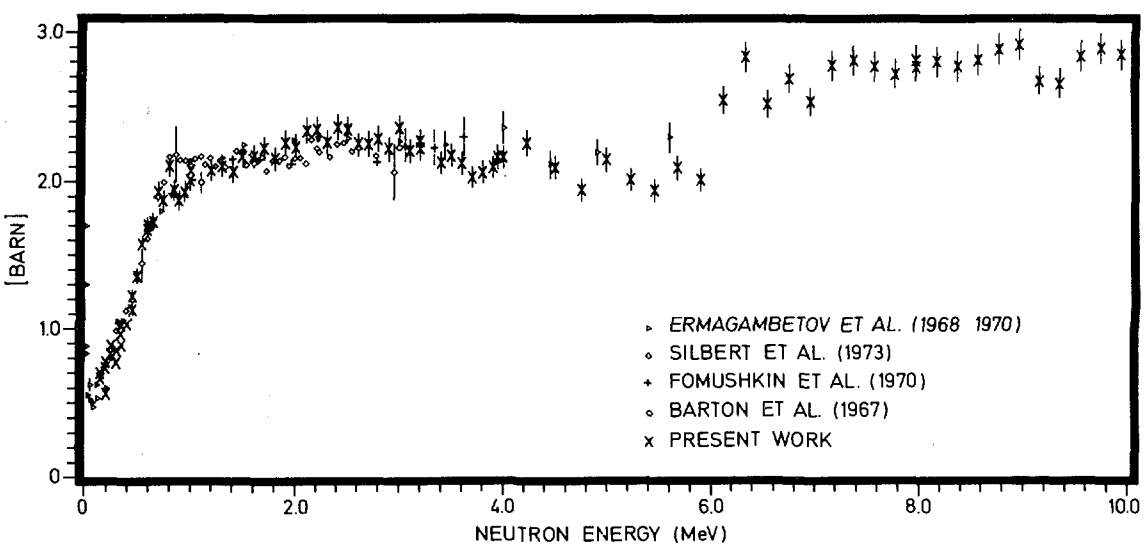

Figure 1.7 Fission cross section of ^{238}Pu from 150 keV to 10 MeV.

The ^{238}Pu-detector with its 47.7 μg of ^{238}Pu was placed at an 8 m station of the linear electron accelerator for measurements in the subthreshold region.

---

* Visiting Scientist from ANL

An energy range from some eV to the MeV region was covered. The sample of ^{238}Pu contains about 10 % of ^{239}Pu, and the fission contribution due to this isotope had to be determined.
This was done by measuring at the same 8 m flight path the time-of-flight spectrum with a sample of ^{239}Pu using the same detector. Fig. 1.8 shows part of the obtained time-of-flight spectra measured with the $^{238+239}Pu$ sample and with the clean ^{239}Pu sample in an energy range from around 50 eV to 1 keV. The contribution from the 10 % ^{239}Pu in the sample can be readily subtracted.

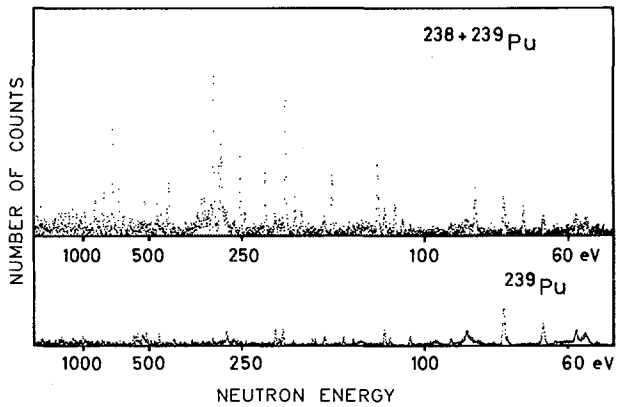

Figure 1.8 Part of the TOF spectra obtained with the $^{238+239}Pu$ sample and with a clean ^{239}Pu sample.

For the evaluation of the cross section data also the neutron spectrum shape below 100 keV neutron energy is needed, since here ^{235}U is not a good standard. This shape is being measured with a ^{6}Li loaded ionization chamber.

Review of ^{240}Pu and ^{242}Pu resolved resonance parameters

H. Weigmann

A paper reviewing the present status of the knowledge of ^{240}Pu and ^{242}Pu resonance parameters has been presented at the IAEA consultants meeting on uranium and plutonium isotope resonance parameters, Vienna, 1981. The main conclusions of this review are that our knowledge of the resonance parameters of ^{240}Pu and ^{242}Pu are adequate for most practical purposes. A few specific problems still exist for ^{242}Pu. There are some uncertainties in the capture widths of ^{242}Pu resonances due to discrepancies in experimental data. Also the neutron widths of a few resonances above 500 eV neutron energy are strongly discrepant. The analysis of the average level spacing of ^{242}Pu has to be checked and probably most evaluations need to be updated with respect to the level spacing and possibly also to quantities derived, when using a low value for the level spacing.

Fission cross section of ^{242}Pu

J.A. Wartena, H. Weigmann, C. Bürkholz

A first series of measurements on the two new samples of ^{242}Pu has been completed at a 25 m flight path station of the linear accelerator. A ^{235}U sample has been used as neutron flux monitor. Considerable structure is observed in the fission yield of ^{242}Pu in the keV neutron energy range. A second series of measurements has been started using a 7 m flight path. The aim of these measurements is to study the energy region below 2 keV with an improved signal to background ratio.

Fission cross section of ^{244}Pu

M.S. Moore★, J.A. Wartena,
H. Weigmann, C. Budtz-Jørgensen,
H.-H. Knitter

The analysis of the fission cross section measurements on ^{244}Pu has been completed. Fig. 1.9 shows the cross section resulting from the present measurements in the MeV neutron energy range (curve 1). To determine the neutron flux the ENDF/B-V data set was used for the fission cross section of ^{235}U. The experimental uncertainty in the MeV energy range is ~ 6 % on the average, which is mainly due to a 5 % normalization uncertainty. Also shown in Fig. 1.9 (curve 2) is the cross section as obtained from the $\sigma(^{244}Pu)/\sigma(^{235}U)$ ratio data of Behrens et al. (1) with the aid of the ENDF/B-V data for $\sigma(^{235}U)$. Although the shapes of the two cross section curves are very similar, the absolute cross section from the present work is on the average 12 % larger than the one of Behrens et al.

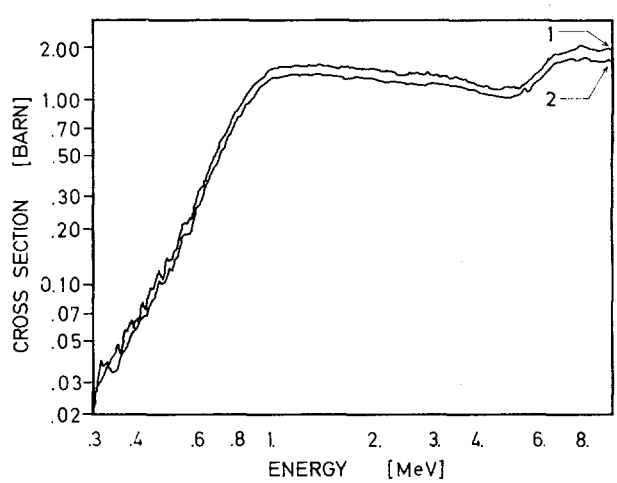

Figure 1.9 Fission cross section of ^{244}Pu
1. present measurements
2. measurements of Behrens et al.

★ Visiting scientist from LASL

(1) J.W. Behrens, R.S. Newburg, J.C. Browne, G.W. Carlson
Lawrence Livermore Laboratory report UCID-17341 (1976)

Below 100 keV neutron energy a number of isolated peaks are observed in the ^{244}Pu fission cross section. Their energies and the integrals A_f of the cross section over the peaks are listed in Table 1.2. The errors given for A_f in Table 1.2 are only the statistical ones to which a 5 % normalization uncertainty has to be added.
The peaks of Table 1.2 are interpreted as being due to individual class II levels, and in most cases probably consist of several unresolved fine structure (class I) resonances. Only the first resonance at 1.65 keV neutron energy can be interpreted as a single isolated fine structure resonance.

Table 1.2
Integrals over low energy peaks in the ^{244}Pu fission cross section (class II areas)

E_n(keV)	A_f(b.eV)
1.6504	35.8 ± 2.0
3.691	9.1 ± 0.9
5.422	4.9 ± 0.8
7.114	9.3 ± 1.1
7.554	11.6 ± 1.2
11.30	7.7 ± 1.3
12.00	12.7 ± 1.6
14.42	37 ± 2.9
15.58	11.9 ± 2.0
17.85	32 ± 2.8
18.26	11.9 ± 1.7
32.7	19.4 ± 2.7
48.9	13.3 ± 3.0
50.8	9.7 ± 2.4
55.8	15.3 ± 3.0
58.5	21.9 ± 4.0
59.7	20.4 ± 3.6
76.4	26.8 ± 3.8
77.2	17.2 ± 3.2
82.2	22.5 ± 4.4

Neutron Capture Cross Section of ^{241}Am

E. Cornelis*, L. Mewissen**,
G. Vanpraet*, J. Wartena,
S. Raman***

The results of the neutron flux measurements with an avalanche detector were not satisfactory. We therefore applied the results of neutron flux determinations with ^{6}Li-glass and ^{10}B slab detectors, as obtained at other flight-paths of the Linac, assuming that the so determined flux shape would be also

* Rijksuniversitair Centrum, Antwerpen, Belgium
** SCK/CEN, Mol, Belgium
*** ORNL

valid in our case. The analysis of the data has been completed and the result is in fairly good agreement with others (Fig. 1.10 and Fig. 1.11).
To improve our data in particular in the unresolved resonance region a new set of measurements has been performed of the average capture cross section of ^{241}Am, using the conventional flux measurement techniques.
The new data are being analysed.

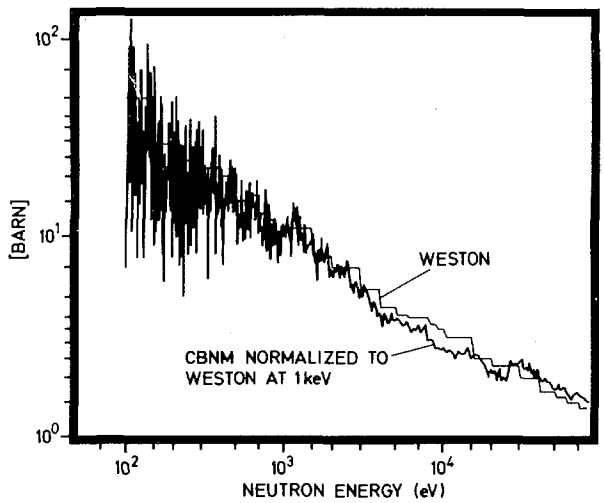

Figure 1.10 ^{241}Am capture cross section.

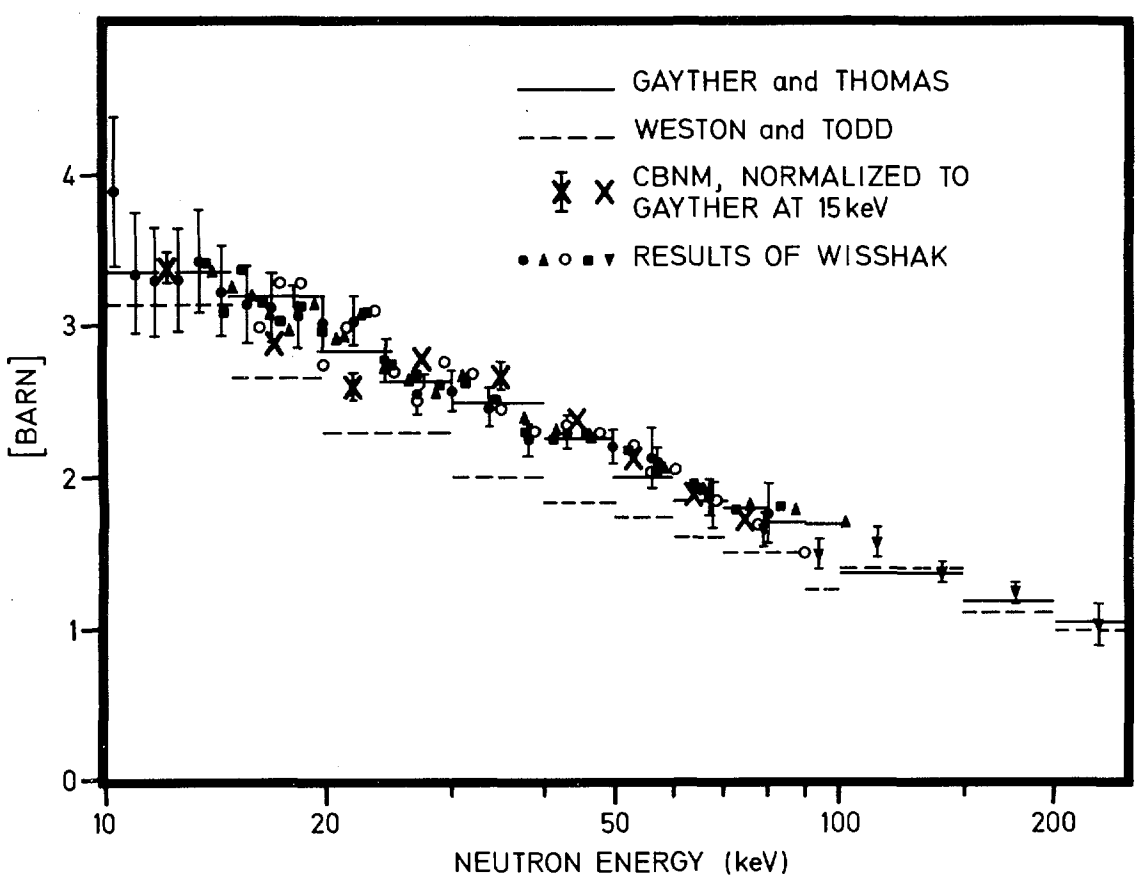

Figure 1.11 ^{241}Am capture cross section.

1.2 CROSS SECTIONS OF STRUCTURAL MATERIAL

High resolution neutron capture cross section of ^{54}Fe

B.J. Allen*, A. Brusegan, F. Corvi, G. Rohr, R. Shelley, T. van der Veen

The analysis of the ^{54}Fe data in the range up to 300 keV has been continued. The background of the time-of-flight spectrum of the capture events decreases monotonically with time and is described by two functions. Below 70 keV the background has been fitted by the function

$$B(t) = C_1 + C_2 \cdot t^{C_3}$$

Due to the broad s-wave resonances ($\Gamma_n \simeq 40$ keV), there are only very few points in the high energy part of the spectrum which are far enough from resonances to be considered as representative of the local background. These points have been interpolated with a linear function of the time-of-flight. First guess-values for the neutron width of the narrow p-wave resonances have been determined with the area analysis programme Tacasi. The shape analysis has been started with the Fanac programme, which was modified as follows:

1. The Gaussian shape for p-wave resonances has been replaced by a single level Breit-Wigner shape.
2. An "effective" mass is used to calculate multiple scattering: i.e. a mass weighted with the isotopic abundance and the scattering cross section for the different materials in the sample.

The Reich-Moore formalism, which is employed in the programme Fanac, was found to be quite inadequate for the analysis of broad s-wave resonances in ^{54}Fe. Energy shifts in the capture resonances were observed and the code generates "ghost" resonances around 175 and 320 keV. The s-wave data were readily fitted by a two channels (one neutron, one capture channel) modification of Fanac.

Preliminary results of the s-wave resonances for the total radiative widths Γ_γ together with the resonance energies and the neutron widths obtained by Cornelis et al. have been collected in Table 1.3.

---

* Visiting Scientist from AAEC Lucas Heights, Australia

Compared to similar measurements at ORELA (Oak Ridge, USA) the contribution of the prompt background in resonances is reduced up to 50 %. The results have been used to check the valence nucleon model:

- The initial state correlation between the s-wave reduced neutron widths and the radiation widths $\rho(\Gamma_{n^\circ},\Gamma_\gamma) = 0.88 \begin{smallmatrix} +0.66 \\ -0.10 \end{smallmatrix}$ where the standard deviation is obtained from Fisher's transformation. This correlation is strongly dependent on the 189 keV resonance and reduces to $0.5 \begin{smallmatrix} +0.23 \\ -0.33 \end{smallmatrix}$ when this resonance is excluded. For the more accurate data below 150 keV, we find no correlation ($\rho = 0.47 \begin{smallmatrix} +0.33 \\ -0.54 \end{smallmatrix}$).
- There are indications that the broad 189 keV resonance (Γ_n = 38.2 keV) interferes destructively with the resonances at 174, 147, 130 and 99 keV, but its asymmetric shape is partly due to the strong multiple scattering effect.

Table 1.3

s-wave resonance parameters

E_n keV	Γ_n keV	Γ_γ* eV
7.74	1.10	1.85 ± 0.19
52.65	1.98	1.53 ± 0.21
71.8	1.68	0.42 ± 0.10
98.7	0.51	1.27 ± 0.13
130.0	3.47	3.21 ± 0.30
147.3	3.78	1.48 ± 0.30
174.0	4.59	0.84 ± 0.30
188.6	38.2	5.30 ± 2.57
223.4	1.08	0.90 ± 0.18
244.1	19.5	2.52 ± 0.69
257.0	0.37	0.89 ± 0.09
291.8	0.89	0.69 ± 0.25

* preliminary values

A new measurement of ^{54}Fe at a flight path length of 30 m has been performed to improve the yield to background ratio for the broad s-wave resonances in order to get better Γ_γ values beyond 150 keV.

Further measurements at the 30 m flight path with a large NaI(Tℓ) crystal are planned to provide more accurate results for the strength of the three highest energy transitions and for the study of the interference effect.

Capture cross section in ^{96}Zr

B.J. Allen*, A. Brusegan, F. Corvi, G. Rohr

Neutron capture cross section measurements in ^{96}Zr were performed at a 62 m flight path in the energy range 0.17 to 90 keV.
The same two C_6F_6 scintillators were used to measure sequentially the flux with a ^{10}B slab, and the capture yield of the Zr sample. The sample was a 13 g of ZrO_2 powder, with a 57.36 % enrichment in ^{96}Zr. Due to the high background and to the important contributions from the other Zr isotopes, the data were only analysed up to about 30 keV. The resonance parameters are deduced by means of an area analysis of the weighted spectra.
For 3 s-wave and 9 p-wave resonances, the capture widths are determined assuming the neutron widths, spin and parity assignments of Coceva et al. (1).
The overall accuracy is estimated to be 20 % including 6 % normalization uncertainty. A paper giving the results and their interpretation in the frame of the valence model of resonance neutron capture is being prepared for presentation at the Grenoble Symposium (7-11 September 1981).
^{96}Zr, having 56 neutrons, a strong p-wave strength function and low lying states of dominant single particle character, appears to be a crucial test of the valence model of resonance neutron capture, i.e. strong valence transitions are expected.
In Table 1.4 resonance parameters are quoted together with the valence neutron transition strength Γ_γ^V calculated for p-wave resonances following the optical model application of Allen and Musgrove (1978) (2).
It can be observed that valence estimates either exceed the observed total radiation widths by a factor of 3 to 5 or are much smaller. Only at 29.81 keV is the valence estimate in agreement with the measured value.
Initial state correlation calculations, which are expected to be significant if the valence component is predominant in the total radiation width, reduce to $\rho(\Gamma_n^1,\Gamma_\gamma) = 0.20 \begin{smallmatrix}+0.37\\-0.44\end{smallmatrix}$ when the 29.8 keV resonance is excluded.
All these results suggest that other capture mechanisms than valence neutron transition must be important in ^{96}Zr.

---

* Visiting Scientist from AAEC Lucas Heights, Australia

(1) C. Coceva, P. Giacobbe, M. Magnani
Resonance Parameters of ^{96}Zr below 40 keV,
Nuclear Cross Sections for Technology, Knoxville, 1979, pag. 319-322

(2) B.J. Allen, A.R. Musgrove
Advances in Nuclear Physics 10, 129 (1978)

Table 1.4

Resonance parameters in ^{96}Zr

E_0(keV)	ℓ	J	Γ_n^1 (eV)*	Γ_γ^V (meV)	Γ_γ (meV)	$\Gamma_\gamma^V/\Gamma_\gamma$
0.301	1	1/2	22.7	631	379 ± 45	1.66
3.818	1	1/2	9.19	249	47 ± 6	5.30
4.132	1	3/2	15.5	302	96 ± 16	3.15
5.443	0	1/2	-	-	62 ± 12	-
5.971	1	3/2	6.93	134	121 ± 21	1.11
9.004	1	1/2	6.39	177	58 ± 15	3.05
13.28	1	1/2	2.16	60	74 ± 20	0.81
15.14	1	(1/2)	2.72	76	470 ± 50	0.16
15.42	0	1/2	-	-	83 ± 24	-
17.78	1	3/2	1.87	36	159 ± 30	0.23
24.69	0	1/2	-	-	60 ± 40	-
29.83	1	3/2	31.3	616	610 ± 140	1.01

* calculated for R = 6.2 fm

1.3 CROSS SECTIONS OF FISSION PRODUCTS

Resonance parameters of Pd isotopes

P. Staveloz**, E. Cornelis***, L. Mewissen*, F. Poortmans*, G. Rohr, R. Shelley, T. van der Veen

This work has been completed. The resonance parameters have been determined up to 2 keV for the uneven isotope ^{105}Pd and up to 20 keV for the even isotopes $^{104,106,108,110}Pd$.

The results for the uneven isotope ^{105}Pd (already reported in a previous report) are:

---

* SCK/CEN, Mol, Belgium.

** I.W.O.N.L. bursary.

*** Rijksuniversitair Centrum, Antwerpen, Belgium.

- average capture width: $\langle \Gamma_\gamma \rangle = (150 \pm 8)$ meV
- s-wave strength function: $S_0 = (0.63 \pm 0.07) \times 10^{-4}$
- s-wave level spacing: $D_0 = (10.0 \pm 0.5)$ eV

For the even isotopes, the results are:

- average capture widths for s-wave resonances:

^{104}Pd	$\langle \Gamma_\gamma \rangle$	=	(80.8 ± 5.0) meV
^{106}Pd	$\langle \Gamma_\gamma \rangle$	=	(62.5 ± 3.4) meV
^{108}Pd	$\langle \Gamma_\gamma \rangle$	=	(54.4 ± 3.2) meV
^{110}Pd	$\langle \Gamma_\gamma \rangle$	=	(54.4 ± 3.6) meV

- The s-wave strength functions:

^{104}Pd	S_0	=	$(0.40 \pm 0.06)\ 10^{-4}$
^{106}Pd	S_0	=	$(0.49 \pm 0.07)\ 10^{-4}$
^{108}Pd	S_0	=	$(0.75 \pm 0.13)\ 10^{-4}$
^{110}Pd	S_0	=	$(0.56 \pm 0.11)\ 10^{-4}$

  The errors quoted are statistical errors, determined by the number of levels observed below 20 keV.

- The s-wave level spacing:

  The set of resonances observed for the even Pd isotopes is an admixture of s-wave and p-wave levels. Only for a limited number of resonances, the l-value could be assigned. The s-wave level spacing has been deduced from a least-squares fit to the distribution of reduced neutron widths. This distribution was taken as a superposition of two Porter-Thomas distributions for s-wave and p-wave levels.

  The following results were obtained:

^{104}Pd	D_0	=	(233 ± 20) eV
^{106}Pd	D_0	=	(220 ± 20) eV
^{108}Pd	D_0	=	(320 ± 30) eV

  The errors quoted for D_0 take into account the statistical errors and the dependence of the results on the bias for the reduced neutron width above which the distribution was fitted.

For ^{110}Pd the fit-procedure yields an unreasonably high value for D_0. This was expected as the distribution of neutron widths showed very strong non-statistical effects. For that nucleus we propose a level spacing deduced from the number of resonances observed, and corrected for the number of missed levels:

^{110}Pd $\quad D_0 = (350 \pm 50)$ eV.

Average capture cross sections of Palladium isotopes

C. Bastian, E. Cornelis*, G. Rohr, G. Vanpraet*

Extending the measurements in the resolved resonance range (see previous annual report) we have started a series of average capture cross section measurements on several Pd isotopes at the 30 m capture facility of fligth path 15. The energy region of interest is between 5 eV and 600 keV. The data have been taken with the newly installed ND 6600 data acquisition system with enlarged memory capacity for bidimensional measurements. Sixteen pulse height groups of 8 K time-of-flight each, were stored for the application of the weighting technique necessary with the C_6D_6 capture γ-detectors. A special effort was made to investigate background contributions in the energy range up to 600 keV. A ^{208}Pb sample (0.5 mm thick) and several black resonance filters were used. The neutron flux was measured with a Li-glass, permanently in the beam, and with a 0.8 mm ^{10}B slab.
All Pd samples, (^{104,105,106,108,110}Pd), have been measured. The new data acquisition system and the analysis procedures will be tested by using results obtained with a 0.5 mm thick Au-sample.

Thermal capture measurements of ^{105}Pd and ^{108}Pd

R. Buyl, F. Corvi

No measured value of the thermal neutron capture cross section of the important fission product ^{105}Pd is reported in the literature. On request of ECN Petten we have undertaken such measurement together with that of ^{108}Pd. Advantage was taken of the enriched samples on loan from ORNL. These samples were previously used at CBNM for neutron resonance parameter determinations (see PPR 1978, 1979 and 1980). The samples are metallic disks of 8 cm diameter with the following characteristics:

^{105}Pd, total weight 7.84 g, enrichment 97.37 %;
^{108}Pd, total weight 22.18 g, enrichment 98.88 %.

The measurements were performed at a 12 m flight distance using two C_6D_6 detectors screened by 10 cm of lead and 10 cm of borated wax. Samples were placed in a ^{6}Li sleeve, 6 mm thick, in order to absorb the scattered neutrons. The background, defined here as the open beam counting rate, was 8 % of the total counting rate of ^{105}Pd and 12 % of that of ^{108}Pd. After appropriate

---

* Rijksuniversitair Centrum, Antwerpen, Belgium

weighting according to signal amplitude, the counting rate of Pd isotopes was compared to that of a 0.1 mm thick gold sample. It was found that the capture cross sections for both isotopes exhibit a 1/v behaviour in the range 0.02 - 0.1 eV. Moreover the values of σ_γ at 0.025 eV were found to be:

$$\sigma_\gamma = 22.0 \pm 1.5 \text{ b for } {}^{105}\text{Pd}$$
$$\sigma_\gamma = 7.28 \pm 0.60 \text{ b for } {}^{108}\text{Pd}$$

The total capture cross section of the element, calculated from the above values plus the data for the other isotopes given in BNL 325, is $\sigma_\gamma = 7.02 \pm 0.50$ b. It is in good agreement with the value $\sigma_\gamma = 6.9 \pm 0.4$ b given in BNL 325.

1.4 GAS PRODUCING REACTIONS

Tritium breeding from ^{7}Li

H. Liskien, A. Paulsen, F. Arnotte, R. Widera

Direct Detection Method.

This work has been finalized. The results and a description of the measurements are summarized in a paper which appeared in Annals of Nuclear Energy 8 (1981) 423. The title reads "Determination of ^{7}Li(n,t) Cross Sections between 6 and 10 MeV". The paper has the following abstract:

"The neutron induced tritium production cross section of ^{7}Li has been determined in view of its relevance to fusion energy applications. Results at 6, 7, 8, 9 and 10 MeV have been obtained by observing tritons emitted from a thin layer. The derived angle-integrated cross sections are typically lower than presently adopted best values."

Activation Method.

Fifteen samples have been irradiated with "quasi-monoenergetic" neutrons of energies between 5 and 8 MeV. Neutrons are produced via the D(d,n)-reaction at 0° using a solid D-Ti target. The neutron flux is determined with a proton recoil telescope positioned at a distance of 50 cm from the source. Corrections for spurious neutrons of lower energy are necessary above 7 MeV. These corrections have been determined using TOF and proton recoil spectrometry and have been found not to exceed 3 %.

The calculation of the neutron fluence averaged over the sample volume takes into account the angular distribution of the source neutrons and the scattering and absorption within the sample. These samples were transported to KFA Jülich, where the quantitative tritium extraction and low level counting is performed in a calibrated anticoincidence proportional counter. Up to now 11 samples have been analysed. The cross section results are given in Fig. 1.12 together with other data not yet available at the time of the ENDF/B-IV evaluation (dashed line). The earlier low result at 7 MeV has not been reproduced and is most probably due to a wrong adjustment of the sample position. Reproducibility checks are going on as well as new measurements at 4.75 and 5.0 MeV.

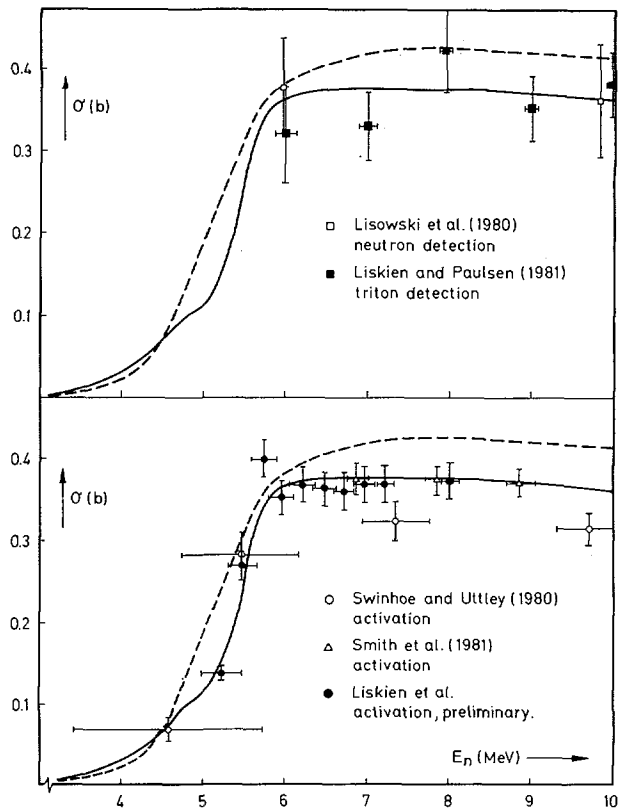

Figure 1.12 ^{7}Li(n,t) results measured by (a) direct detection and (b) by activation together with other results not yet available at the time of the ENDF/B-IV evaluation (dashed line). The other curve (full line) is a recent LA-evaluation.[1]

Measurements of (n,α) cross sections at 14 MeV

E. Wattecamps, F. Arnotte

Measurements have been made at the 7 MV Van de Graaff accelerator for elemental Fe, Cr, and Ni using D(d,n)-neutrons in the energy range from 5 to 10 MeV [2]. The neutron target and the multi-telescope were adapted for similar measurements with 14 MeV T(d,n)-neutrons.

(1) P.G. Young, LA-8874-PR(1981) p.2

(2) A. Paulsen et al.
NSE 78, 377 (1981)

To get benefit of the large T(d,n) cross section at 110 keV a thick target of 4 mg/cm^2 T-Ti tilted by 45° was used and bombarded with deuterons of 1 MeV, which is the lowest energy available with our accelerator. This target yields $1.7 \cdot 10^7$ neutrons/(sr.μCb) of 14 MeV and withstands the available 15 μA. These figures are to be compared with those of the earlier used gas target which delivered $1.5 \cdot 10^8$ neutrons/(sr.μCb) of 8 MeV at the maximum current of 4 μA. However, the increased neutron energy results in a much larger background of spurious charged particles than earlier seen. This background has been reduced by two means: (a) the time resolution has been brought down from 175 ns to 50 ns by otimizing the position and diameter of the counting wires, (b) the charged particle background has been reduced by minimizing the counting volumes of the proportional counters and by replacing remaining low-Z material inside the chamber by tantalum.

1.5 VARIOUS MEASUREMENTS

Thick-Target ^{9}Be(d,n)^{10}B spectrum

A. Crametz, H.-H. Knitter, D.L. Smith*

The determination of the shape of the neutron spectrum produced by 7-MeV deuteron bombardment of a 0.5 mm thick wafer of beryllium has been completed for the range E_n = 0.7 MeV to the endpoint at 11.4 MeV (defined by the reaction Q-value). Formulas for generating a complete covariance matrix for the spectrum were developed to consider the relative efficiency of the scintillation detector, the time-of-flight parameters and statistics.
In order to demonstrate the usefulness of this source we measured total cross sections, using the thick-target ^{9}Be(d,n)^{10}B spectrum as a white source, and time-of-flight techniques to establish the energy scale. Data were obtained for carbon and silicon. Our results are shown in Figs. 1.13 and 1.14 and they are seen to agree well with ENDF/B-V values. Due to the intensity of this source, we were able to measure the cross sections for both these elements from ~ 1 to 10 MeV in less than 16 hours.

---

* Visiting Scientist from ANL

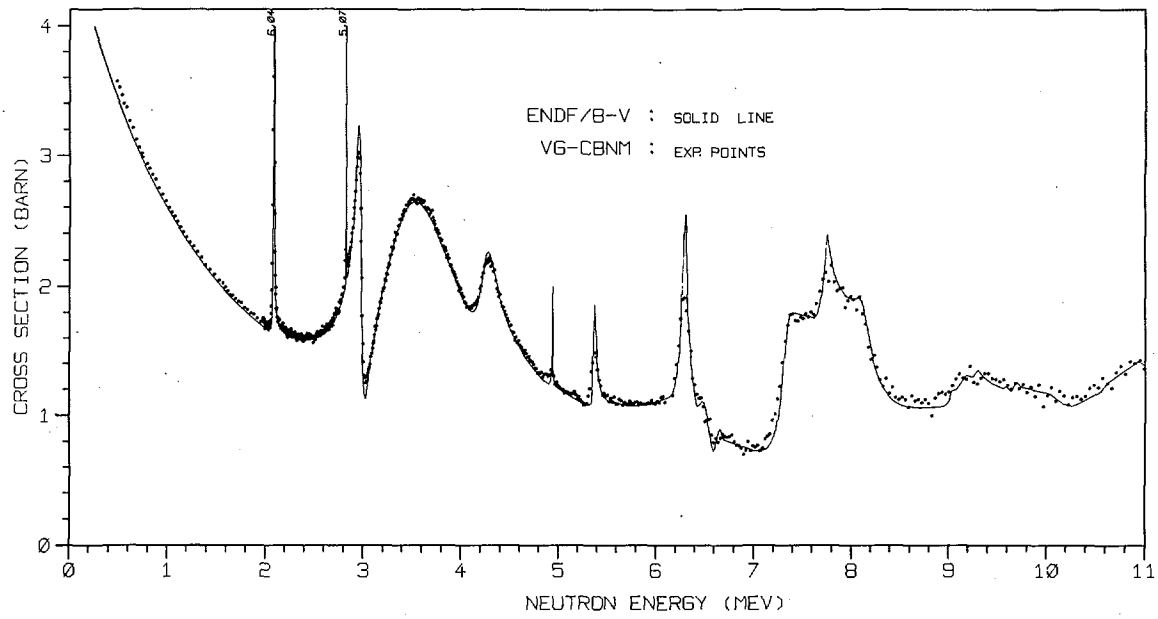

Figure 1.13 Total cross section of ^{12}C.

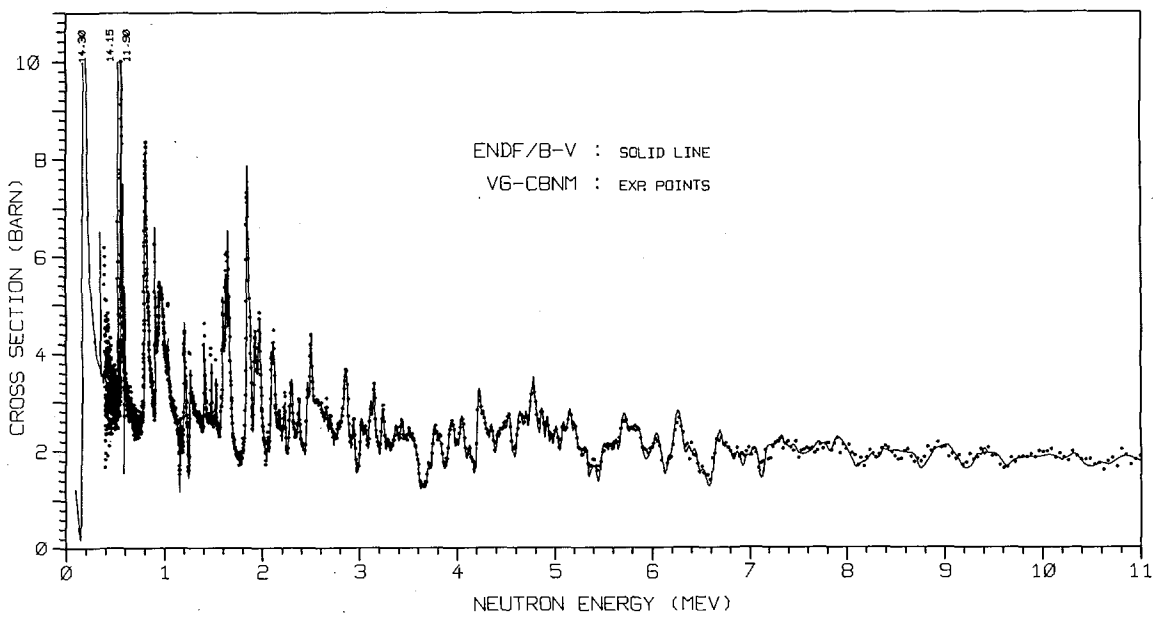

Figure 1.14 Total cross section of ^{28}Si.

Neutron energy spectra from (α,n) reactions in light elements

G. Jacobs*, H. Liskien

Neutron energy spectra from (α,n) reactions on thick targets are determined with a calibrated neutron spectrometer based on NE-213 liquid scintillation using time-of-flight techniques. For each target and for each α-energy, measurements were performed at five different angles relative to the incident α-particle beam (0°, 30°, 60°, 90°, 140°). To permit correction for the neutron background each foreground measurement is accompanied by a measurement where a shadow cone is inserted between the target and the neutron spectrometer. With this shadow cone all neutrons directly coming from the target are removed from the spectrum, so only scattered neutrons are registered.

As an example, the neutron energy spectra determined at the five emission angles are presented in Fig. 1.15 for a thick aluminium target bombarded with 5.50 MeV α-particles. For energies smaller than 300 keV the spectra had to be extrapolated. These five angle differential spectra show a gross structure, which corresponds to the nuclear levels of the product nucleus and a fine structure due to the levels in the compound system. The angle-integrated neutron energy spectrum, the interesting one for practical use, is shown in the lower part of Fig. 1.15 and was obtained as described below:

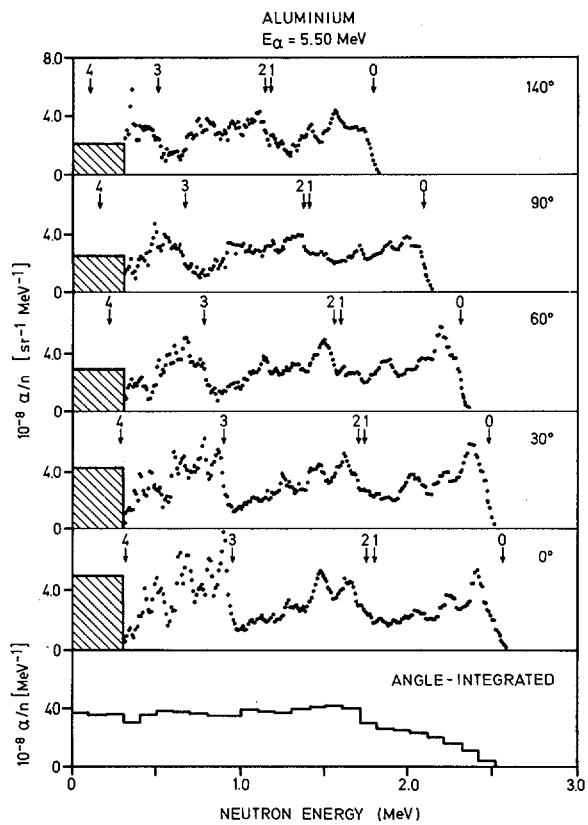

Figure 1.15 Neutron energy spectra at five measured angles with respect to the incident α-direction. At each angle the maximum neutron energies, resulting from (α,n) reaction, that leave the product nucleus in different excited states are indicated by 0,1,2,3 and 4.
The angle-integrated spectrum is the bottom part of the figure.

---

* Bursary of the European Community

To solve the problem correctly, the relation to thin-target measurements has been made. The thick target is assumed to be composed of a number of "thin targets", such that the energy loss in any of the "thin target", ΔE_α, is the same. First, for each "thin target" and any of the five selected neutron observation angles the boundaries of the kinematically allowed neutron energy interval were determined using the Q-equation and the stepwise decreasing α-particle energy. Then, a Legendre polynomial fit of the contents of the so determined neutron intervals is performed. This fit is now used to determine the contribution of each "thin target" to the neutron energy spectrum at laboratory angles with $\cos \Theta_n = 0.9, 0.7, \ldots, -0.7, -0.9$. The neutron energy intervals at these angles are again determined by the Q-equation. Finally, the various contributions for each "thin target" and each $\cos \Theta_n$ are sorted into neutron energy groups with constant meshes. In this way neutron energy spectra are calculated at angles with cosinus equidistantly spread. Integration within each energy group using a step-function determined by the contents at the ten angles results is a good approximation of the angle-integrated neutron energy spectrum.

Table 1.5 gives a survey of the materials and α-particle energies for which spectra were obtained. The preliminary n/α-values result from integration of the angle-integrated spectra. They are within the experimental uncertainties in agreement with literature values, obtained by measurements with large moderators.

Table 1.5

Number of neutrons per incident α-particle (n/α)

E_α (MeV) \ target material	C	Mg	Al	Si
4.0	$4.7\ 10^{-8}$	$7.5\ 10^{-7}$	--	$3.0\ 10^{-9}$
4.5	$5.1\ 10^{-8}$	$2.8\ 10^{-7}$	$9.0\ 10^{-8}$	$1.2\ 10^{-8}$
5.0	$6.3\ 10^{-8}$	$6.7\ 10^{-7}$	$2.8\ 10^{-7}$	$4.5\ 10^{-8}$
5.5	$10.5\ 10^{-8}$	$13.2\ 10^{-7}$	$7.6\ 10^{-7}$	$10.4\ 10^{-8}$

The measurements for C, Mg, Al, Si have then been extended to the compounds Al_2O_3, SiO_2 and BN, using the same equipment and the same measuring procedure and analysis. The neutron energy spectra obtained for BN are given in Fig. 1.16.

The choice of the compounds has been guided by their direct importance for waste treatment (Al_2O_3, SiO_2) and by the possibility to obtain spectra for the elements forming the compound. Assuming an identical shape for the stopping power of different elements as function of the α-particle energy, results in a linear relation between the spectrum of a compound and the spectra of the elements forming the chemical compound. This allows the extension of the measurements to elements which are not easy to handle as target material. As an example the angle-integrated thick-target neutron spectrum for oxygen and 4.0 MeV α-particle energy is given in Fig. 1.17. The results obtained from the spectra of Al and Al_2O_3, and from the spectra of Si and SiO_2 are in good agreement.

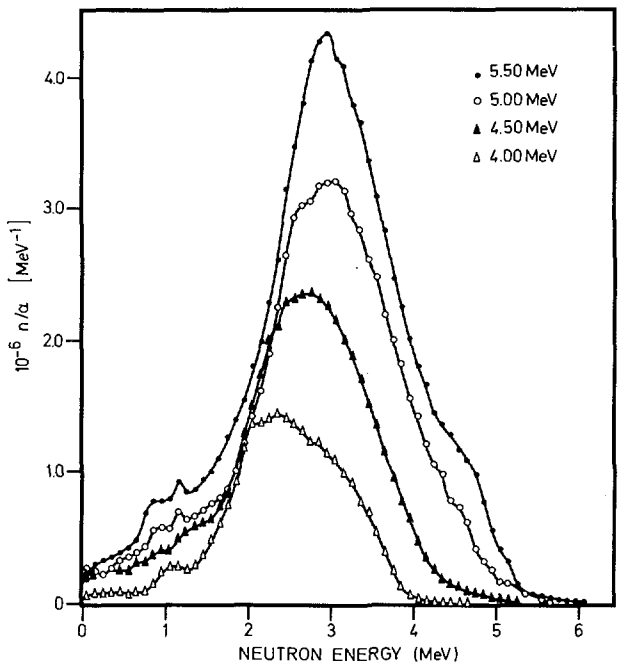

Figure 1.16 Angle-integrated neutron energy spectra for a thick boronnitride target when bombarded with α-particles of 4.0, 4.5, 5.0, 5.5 MeV energy.

Neutron Resonance Parameters of ^{32}S

C.R. Jungmann***, E. Cornelis**,
L. Mewissen*, F. Poortmans*,
H. Weigmann

The analysis of the high resolution total cross section and differential elastic scattering experiments is completed. The neutron widths of the resonances are obtained from a multi-level-Breit-Wigner analysis of the total cross section data. The spin and parity of most of the resonances could be determined from the angular distribution of the elastically scattered neutrons. An example of the resonance shapes for six scattering angles for the energy range from 640 keV up to 750 keV is shown in Fig. 1.18.
The results are summarized in Table 1.6.

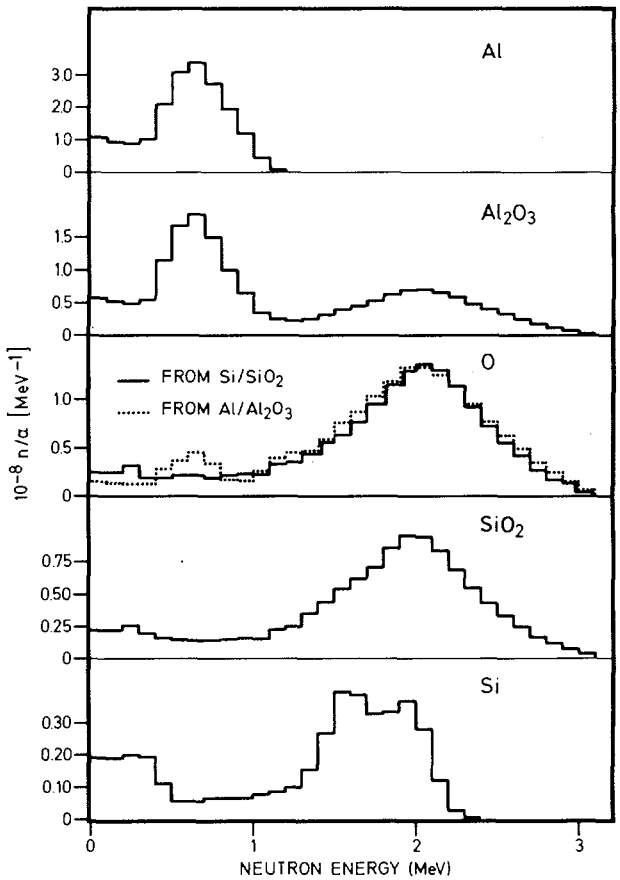

Figure 1.17 Angle-integrated neutron energy spectra for a thick target of aluminium, aluminiumoxide, silicon, and siliconoxide when bombarded with 4.0 MeV α-particles. The spectra for oxygen have been deduced from the measured spectra.

For isolated resonances with a neutron width larger than the resolution width, the statistical weight factors $g = (2J+1)/2(2I+1)$ and so the resonance spin values J could be determined from the experimental peak total cross section of the resonances. They are all in agreement with the results from the scattering experiments.
The resonance parameters obtained from the analysis of high resolution total cross section and differential elastic scattering data on ^{32}S have been compared to theoretical calculations by Halderson et al. (1).

---

* SCK/CEN, Mol, Belgium
** Rijksuniversitair Centrum, Antwerpen, Belgium
*** Bursary of the European Community

(1) D. Halderson, B. Castel, G. Aizer
J. Phys. G6, 59 (1980), and private communication

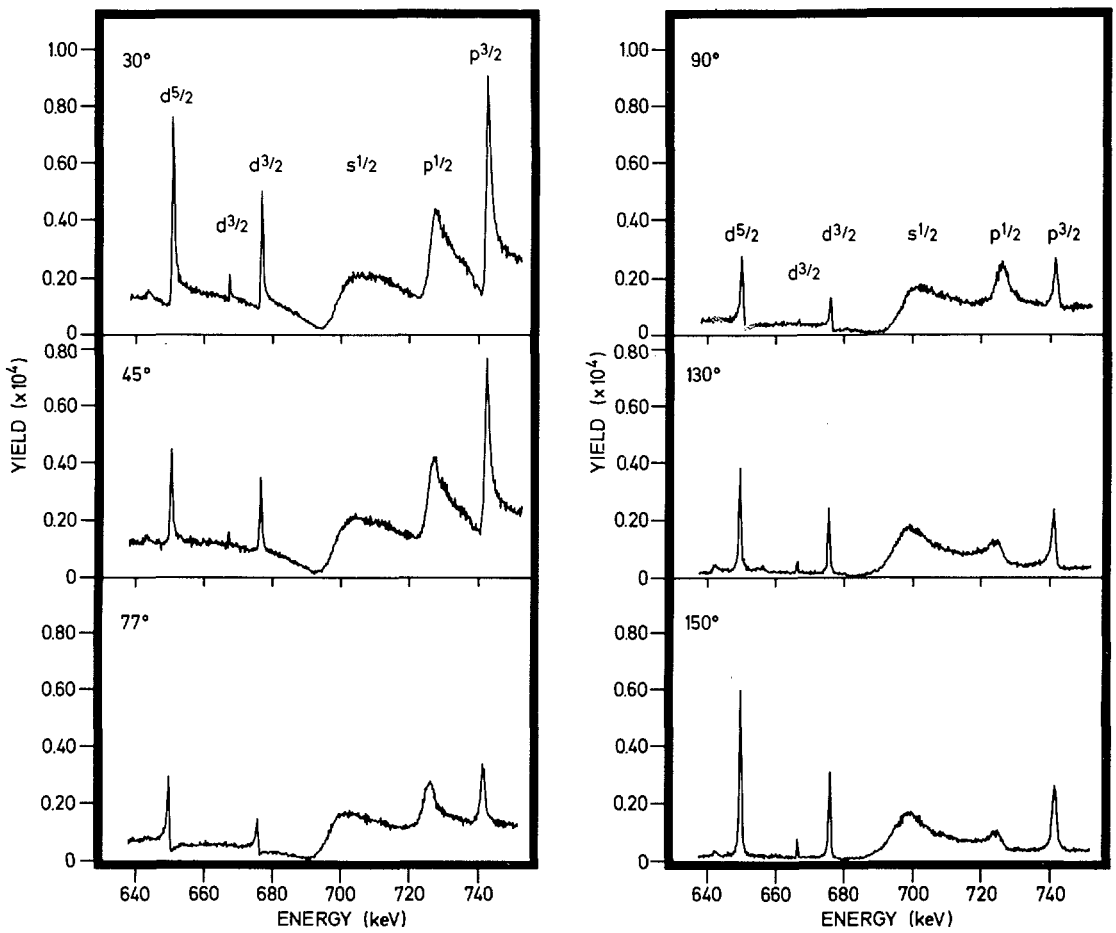

Figure 1.18 Yields of neutrons elastically scattered by ^{32}S at laboratory angles between 30° and 150°.

These calculations use a particle plus vibration model for the negative parity states and a particle-hole picture for the positive parity ones. A comparison of the number of levels predicted in the calculations with the experimental ones shows reasonable agreement for the positive parity levels, whereas the number of negative parity levels is strongly under-predicted by the pure particle plus vibration model. However, in spite of this fact it is still worthwhile to compare the calculated strength of predicted simple states with the experimental one in the same energy region: the doorway character of the simple configurations would insure that their strength is merely distributed over a larger number of levels.

Table 1.6

The first column gives the fitted resonance-energies followed by the experimental uncertainties for these energies. The resonance parameters ℓ and J are mostly obtained from the elastic scattering. Then follows the neutron-width multiplied by the g-factor $g\Gamma_n$ from the fit to the transmission. The error arises from the statistical uncertainty of the measurement. Next is the neutron-width Γ_n and the reduced neutron-width $\Gamma_n^{(\ell)}$, which corresponds to an assumed interaction-radius of 4.7 fm. For the f-waves, the values in strokes give $g\Gamma_n^{(\ell)}$. Whenever the ℓ or J assignment is doubtful, the value is put in square brackets. Members of a multiplet are marked with an asteriks.

Resonance Energy (keV)	Uncertainty (keV)	ℓ	J	$g\Gamma_n$ (eV)	Error (eV)	Γ_n (eV)	$\Gamma_n^{(\ell)}$ (eV)
203.44	0.04	1	1/2	3119.8	12.	3119.8	41.02
261.28	0.04	2	5/2	11.8	1.2	3.9	1.1
272.38	0.04	1	1/2	1628.	9.	1628.	14.57
288.66	0.05	1	3/2	2284.	8.	1142.	9.49
309.38	0.05	[2	5/2]	22.8	2.1	7.6	1.43
321.33	0.05			5.6	1.2		
346.03	0.06	1	3/2	43.4	1.	21.7	0.14
353.57	0.06	2	5/2	20.7	0.9	6.9	0.94
376.99	0.06	0	1/2	7969.	14.	7969.	12.98
378.87	0.06	> 1		18.8	1.6		
401.39	0.07	> 1		13.6	1.		
412.68	0.07	1	3/2	148.	2.8	74.	0.39
460.02	0.08	2	3/2	108.	2.6	54.	3.98
463.12	0.08	2	5/2	252.	3.	84.	6.1
513.73	0.09	> 1		26.6	1.9		
533.39	0.10	> 1		28.7	1.1		
576.34	0.11	> 1		20.4	2.2		
★ 586.54	0.11	1	[3/2]	322.	12.	161.	0.57
★ 587.37	0.11	2	5/2	3855.	18.	1285.	53.98
646.2	0.13	> 1		18.5	4.6		
649.76	0.13	2	5/2	1509.	11.	503.	16.81
666.52	0.13	2	3/2	62.4	3.2	31.2	0.98
675.92	0.14	2	3/2	830.	16.	415.	12.69
696.08	0.14	0	1/2	11279.	88.	11279.	13.52
726.00	0.15	1	1/2	3779.	49.	3779.	10.54
741.58	0.16	1	3/2	2514.	32.	1257.	3.43
★ 776.80	0.17	3		171.	36.		/109.21/
★ 779.42	0.17	1	3/2	2954.	56.	1477.	3.82
★ 784.38	0.17	2	3/2	296.	24.	148.	3.25
791.95	0.17	2	3/2	48.	4.	24.	0.52
819.35	0.18	2	5/2	1764.	15.	588.	11.73
834.33	0.18	3		243.	9.		/122.44/
866.48	0.19	> 1		50.7	4.		
869.46	0.19			50.1	4.		
885.25	0.2	3		237.	6.		/ 98.12/
901.85	0.2	> 1		123.6	6.		
★ 920.54	0.21	2	5/2	2142.	75.	714.	11.07
★ 921.69	0.21	1	3/2	6020.	110.	3010.	6.54
947.88	0.22	2	5/2	3270.	36.	1090.	15.88
986.58	0.23	1	1/2	6948.	184.	6948.	15.73

Table 1.6 (Continued)

Resonance Energy (keV)	Uncer-tainty (keV)	ℓ	J	$g\Gamma_n$ (eV)	Error (eV)	Γ_n (eV)	$\Gamma_n^{(\ell)}$ (eV)
1008.8	0.24	1	[3/2]	1608.	58.	804.	1.59
★1045.6	0.25	3		208.5	25.5		/ 49.8 /
★1047.5	0.25	0	1/2	1556.	83.	1556.	1.52
★1049.7	0.25	1	[1/2]	2991.	114.	2991.	5.70
★1056.2	0.26	2	5/2	4668.	99.	1556.	18.03
1065.9	0.26	0	1/2	276.	21.	276.	0.27
1068.0	0.26	> 1		31.2	20.1		
1085.2	0.27	3		302.1	27.3		/ 64.01/
1088.0	0.27	> 1		66.4	20.		
1092.4	0.27	1	3/2	875.6	27.6	437.8	0.8
1107.7	0.27			32.2	13.8		
1115.4	0.28	1	3/2	1620.	60.	810.	1.45
1140.7	0.28	1	1/2	1544.	66.	1544.	2.71
1150.9	0.29	2		159.	22.2		0.22
1161.4	0.29	0	1/2	1233.	112.	1233.	1.14
1165.8	0.29	2	3/2	858.	75.	429.	4.05
1174.5	0.3	3		370.5	26.		/ 60.72/
1204.0	0.3	1	3/2	684.4	23.4	342.2	0.57
1219.0	0.31	2	3/2	2556.	50.	1278.	11.02
★1242.0	0.32	[3	7/2]	10904.	252.	2726.	372.7 /1490.8 /
★1244.9	0.32	1	[3/2]	2406.	190.	1203.	1.94
1255.7	0.33	3	[5/2]	1374.	54.	458.	60.49 / 181.46/
1275.8	0.33	1	3/2	6334.	170.	3167.	5.0
1290.0	0.34	0	1/2	10975.	654.	10975.	9.65
1307.4	0.35	2	3/2	394.	50.	197.	1.48
1324.7	0.35	2	5/2	1122.	84.	374.	2.73
1340.2	0.36	2	5/2	4767.	90.	1589.	11.32
1352.2	0.36			172.5	47.		
1360.7	0.37	3	7/2	5068.	116.	1267.	129.28 / 517.14/
1378.5	0.37	2	5/2	341.1	105.	113.7	0.77
1385.0	0.38	1	3/2	5510.	78.	2755.	4.03
★1398.2	0.38	1	1/2	681.	55.	681.	0.99
★1401.1	0.38	2	5/2	1116.	51.	372.	2.43
1419.4	0.39	0	1/2	873.	133.	873.	0.73
1426.1	0.39	1	3/2	6120.	124.	3060.	4.36
1456.1	0.4	3		756.6	33.		/ 62.21/
1474.1	0.41						
1480.0	0.41						
1487.3	0.42						
1525.9	0.43	2	3/2	8146.	180.	4073.	22.52
1534.5★	0.44	> 0		527.6	73.2		
1537.8★	0.44	> 1		3726.	123.		
★1563.9	0.45	3		602.7	97.		/ 39.54/
★1571.1	0.45	2	[5/2]	2898.	129.	966.	5.05
1587.3	0.46	[DOUB.]		9237.	756.		
1605.6	0.47	0	1/2	602.1	247.	602.	0.48
1625.2	0.47	2	5/2	22092.	831.	7364.	36.11
1659.4	0.49	0	1/2	2785.	268.	2785.	2.16
1700.0	0.51		END OF PARAMETER ANALYSIS				

For the purpose of such a comparison, in Figures 1.19a and 1.19b the cumulative sums of the experimental reduced widths are plotted together with the theoretical ones of Halderson et al., for each compound spin separately.

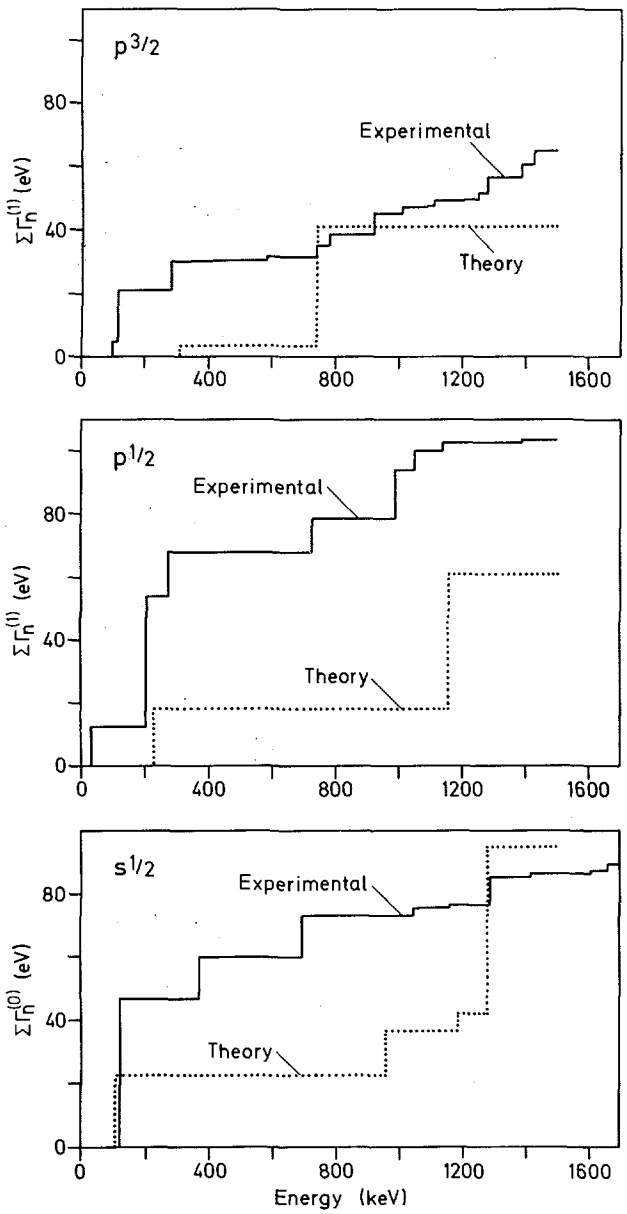

Figure 1.19a Comparison of cumulation sums of calculated and experimental reduced widths for s- and p- wave resonances.

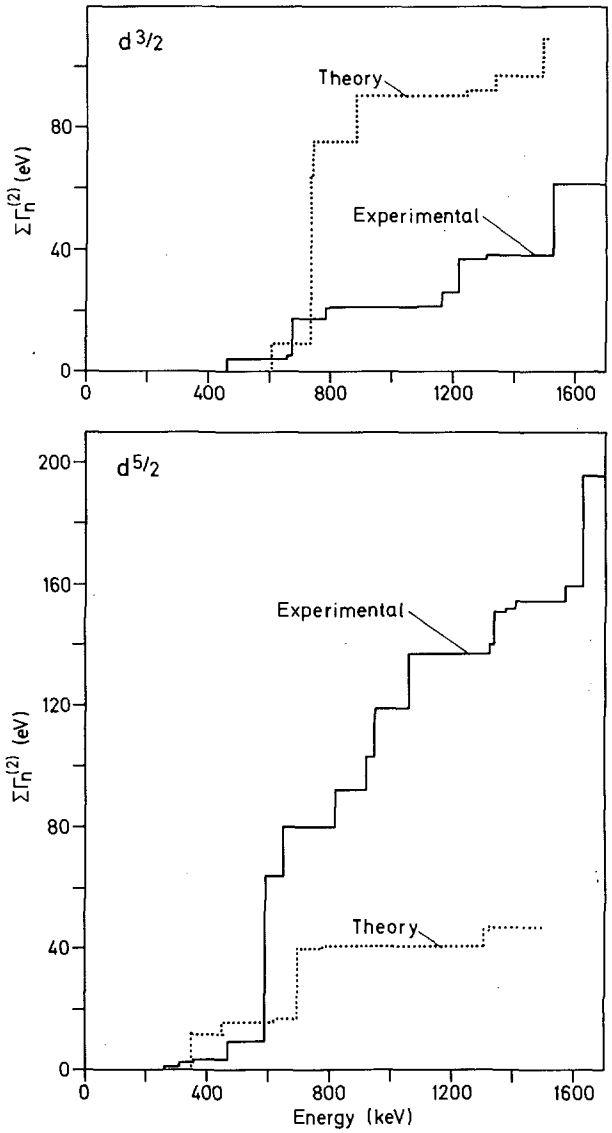

Figure 1.19b Comparison of cumulative sums of calculated and experimental reduced widths for d-wave resonances.

The position of the calculated levels is uncertain to approximately 0.5 MeV [1]. For that reason, there is generally little similarity between the staircase-functions representing experiment and theory in Figs. 1.19a and 1.19b. However the total strengths in the energy range investigated coincide to within 50 % on the average for the s- and p-waves, but the agreement is not so good for the d-wave resonances. Fig. 1.20 shows the cumulative sum of experimental $g\Gamma_n^{(3)}$-values for f-wave resonances. The broken line results if the resonance at 1242 keV neutron energy, the f-wave assignment of which is doubtful, is included in the data set.

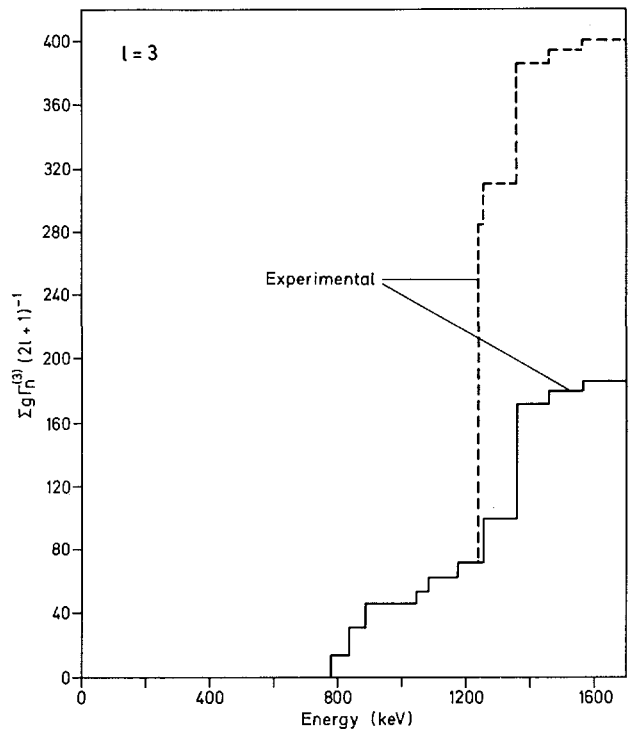

Figure 1.20 Cumulative sum of experimental $g\Gamma_n^{(3)}$-values for f-wave resonances. The broken line results if the resonance at 1242.2 keV is included.

From the cumulative sums of experimental reduced widths we have calculated strength functions for each compound spin according to

$$S(J^\pi) = \langle \Gamma_n^{(\ell)} (J^\pi) \rangle / D (J^\pi)$$

The resulting values are given in column 2 of Table 1.7. For f-wave resonances where no spin assignments have been attempted, only the overall $\ell = 3$ strength function is given; the entry in brackets results if the resonance at 1242 keV is included in the set of f-wave resonances.

For comparison, in column 3 of the table we also list strength functions obtained for 1 MeV neutron energy from an optical model calculation with the code CERBERO-3 of Fabbri et al. [2], using the standard optical model parameter set of Igarasi et al. [3].

---

(1) D. Halderson, B. Castel, G. Aizer
J. Phys. G 6, 59 (1980), and private communication

(2) F. Fabbri, G. Fratamico, G. Reffo
CNEN-Report RT/FI (77) 6, 1977

(3) S.G. Igarasi et al.
Report JAERI 1228, 41 (1974)

The agreement is surprisingly good for positive parity, whereas the p-wave strength functions disagree by a factor of about 2.5.
In the range of excitation energies in ^{33}S covered by the present measurements, several T = 3/2 levels are expected. One of them, the analogue to the 3.49 MeV ($5/2^+$) level in the parent nucleus ^{33}P, has been identified as the resonance at 353.57 keV neutron energy. From the neutron width of this resonance an estimate of the isospin mixing matrix element of ~ 18 keV has been obtained.
For a second T = 3/2 level, analogue of the 4.048 MeV ($3/2^+$ or $5/2^+$) level in ^{33}P, two candidates have been found, i.e. the resonances at 901.85 keV and 920.54 keV neutron energy.
Depending on which resonance is to be identified with the T = 3/2 level and on the spin of that level, isospin mixing matrix elements between 4 keV and 35 keV would result.
The order of magnitude of isospin mixing matrix elements obtained fits into systematics known from neighbouring nuclei.

Table 1.7

Strength functions for $^{32}S+n$

J^π	$S(J^\pi)$ [10^{-4}]	
	experim.	optical model
$1/2^+$	$0.56^{+0.37}_{-0.20}$	0.53
$1/2^-$	$0.72^{+0.56}_{-0.36}$	1.88
$3/2^-$	$0.48^{+0.21}_{-0.13}$	1.17
$3/2^+$	$0.55^{+0.36}_{-0.19}$	0.68
$5/2^+$	$1.40^{+0.63}_{-0.39}$	1.44
$\ell = 3$	$2.29^{+1.51}_{-0.81}$ $(4.97^{+3.12}_{-1.67})$	2.18

The $^{33}S(n,\alpha)$ reaction in the resonance region

C. Wagemans*, H. Weigmann, R. Barthélémy

A first series of measurements on the $^{33}S(n,\alpha)^{30}Si$ reaction has been started. Fig. 1.21 shows preliminary results obtained in the neutron energy region from 5 keV to 400 keV. At lower energies no resonances have been observed.

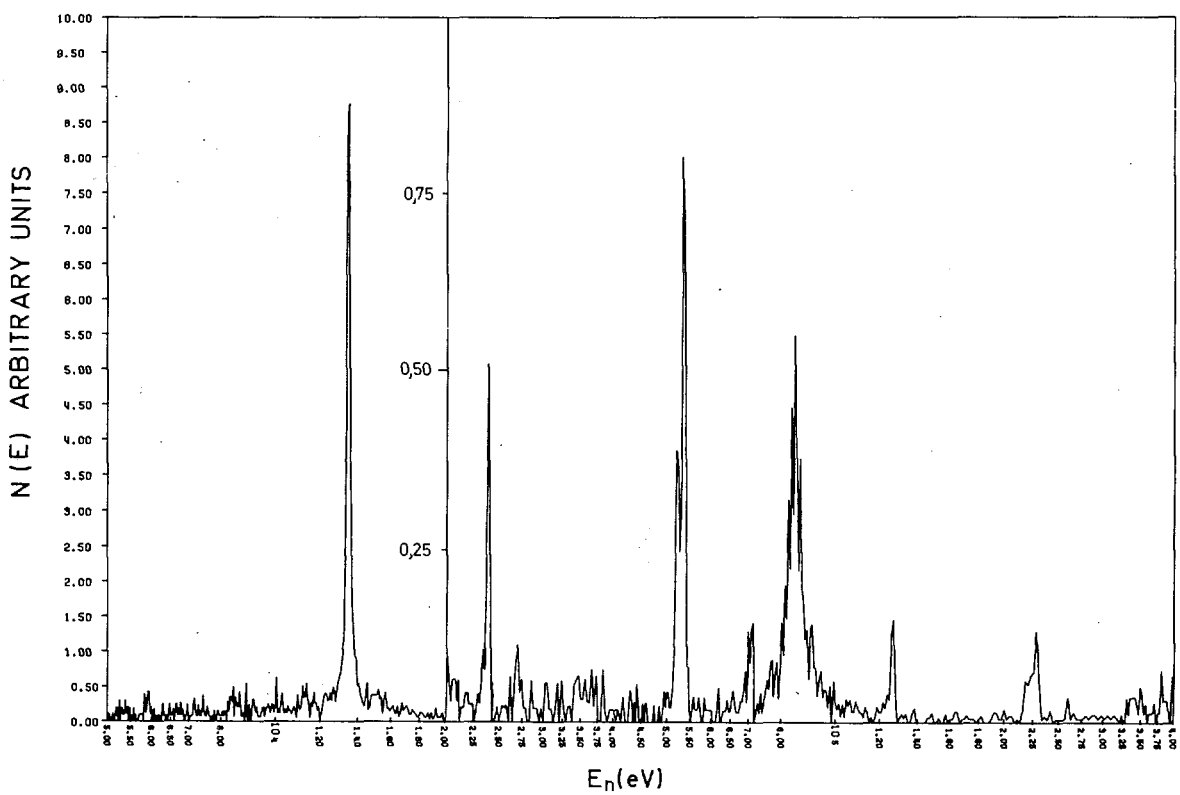

Figure 1.21 The $^{33}S(n,\alpha)$ cross-section for neutron energies from 5 to 400 keV.

Above 50 keV the experimental resolution was insufficient to separate all resonances. To improve this and to investigate the $^{33}S(n,\alpha)^{30}Si$ reaction at higher neutron energies, a higher resolution experiment is in preparation.

---

* SCK/CEN Mol and RU Gent, Belgium

Neutron induced charged particle reactions on ^{40}K

H. Weigmann, C. Wagemans*, R. Barthélémy, A. Emsallem**, M. Asghar***

This work has been finished and a paper has been prepared for publication. The abstract is as follows:

"The $^{40}K(n,\alpha)^{37}Cl$ and $^{40}K(n,p)^{40}Ar$ reaction cross sections were measured in the neutron energy region from 0.02 eV up to about 70 keV. The proton and alpha-particles were detected with a large surface barrier detector, and the neutron energy was measured by time-of-flight. The reaction cross sections show a pronounced resonance structure. A comparison of the density of s- and p-wave resonances (compound spins between 5/2 and 11/2) in $^{40}K+n$ to the density of spin 1/2 compound states observed as resonances in the reaction $^{40}Ar+p$ by Keyworth et al., allows a direct determination of the spin cut-off parameter of the level density."

The neutron capture mechanism in ^{88}Sr

B.J. Allen+, R. Shelley, T. van der Veen, A. Brusegan, G. Rohr, G. Vanpraet++

In an earlier capture measurement (Boldeman et al. 1976), a strong correlation between the p-wave reduced neutron widths and the corresponding radiation widths was observed and interpreted as a consequence of the valence model. The low lying states of ^{89}Sr have a strong single particle character and the predicted valence capture spectra are dominated by only a few transitions. Valence interference effects might therefore be observed in the resonance capture cross section for the strong p-wave resonances near 300 and 550 keV. Two measurements of the resonance capture yields on a highly enriched $Sr(NO_3)_2$ sample were made at a 60 m station of the Geel electron linear accelerator with C_6D_6 detectors using the pulse height weighting method.

The time-of-flight spectrum below 400 keV was first measured with the moderated neutron target, and later with the bare target assembly to obtain improved statistics at higher neutron energies.

---

* SCK/CEN Mol and RU Gent, Belgium

** IPN - Lyon, France

*** ILL - Grenoble, France

+ Visiting Scientist from AAEC Lucas Heights, Australia

++ Rijksuniversitair Centrum, Antwerpen, Belgium

Neutron flux measurements were made with ^{6}Li glass and ^{10}B slab techniques, and in a separate measurement the capture data were normalized to the 1.152 keV resonance in ^{56}Fe. High bias data were also taken to obtain more specific information on the high energy component of the γ-ray resonance yields.

Capture data are being analysed by TACASI and FANAC Codes and results compared with those of Boldeman et al. (1976). We reproduce very well their energy scale and find in the low energy region, agreement in capture areas. At high energies discrepancies occur for individual resonances. In general our data have superior resolution and a substantially lower prompt background.

Correlations between the reduced neutron widths of p 1/2, p 3/2 and s 1/2 resonances and their corresponding radiation widths have been calculated and uncertainties are derived from Fisher's transformation. The large correlation of Boldeman et al. for p 3/2 resonances is not reproduced for valence neutron capture.

Resonance capture yields on a highly enriched $Sr(NO_3)_2$ sample did not reproduce large correlations between the reduced neutron widths of the p 3/2 resonances and their corresponding radiation width below 330 keV. The discrepancies with earlier capture measurements (Boldeman et al. 1976), suggesting a deficiency in valence strength, were explained as being due to an underestimate in the Boldeman results of the prompt background correction for these resonances with large scattering widths.

Our analysis of these resonances has been performed with single level Breit-Wigner fits using the neutron width of Boldeman et al. Because of destructive interference in the total cross section, a multilevel calculation is required to obtain the correct multiple scattering contribution to the capture yield. The observed yields appear to be consistent with an interference effect, but the statistics are inadequate for a definitive statement to be made.

1.6 STANDARD NEUTRON DATA

$^{6}Li(n,\alpha)/^{10}B(n,\alpha)$ cross section ratio: feasibility study with a Xe scintillator

C. Bastian, H. Riemenschneider

The principle of detection inside of hollow cylindrical samples was kept (Fig. 1.22). The set-up was thoroughly modified to simplify the sample changer in the xenon container and to improve the signal/noise ratio for low energy reaction products. The scintillation properties were studied using the spontaneous α-emission of the uranium coated sample. It turned out that the optimum light yield can be maintained by circulating the gas continuously through a purifier (titanium oven). Under these conditions, the products of $^{6}Li(n,\alpha)$ and $^{10}B(n,\alpha)$ reactions induced by the neutron beam in the two other samples could be detected (Fig. 1.23), but not fully separated.

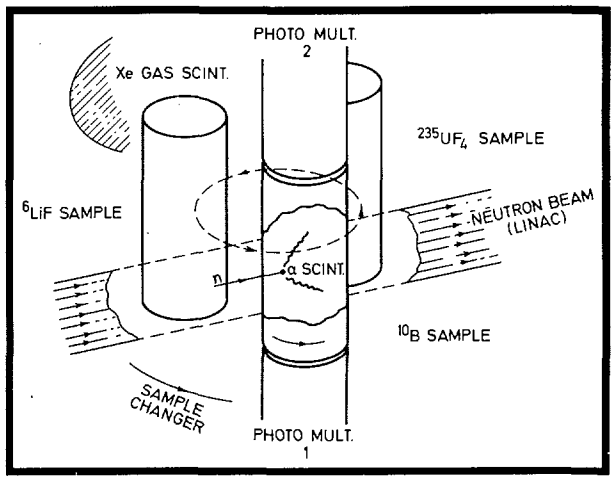

Figure 1.22 Detector set-up.

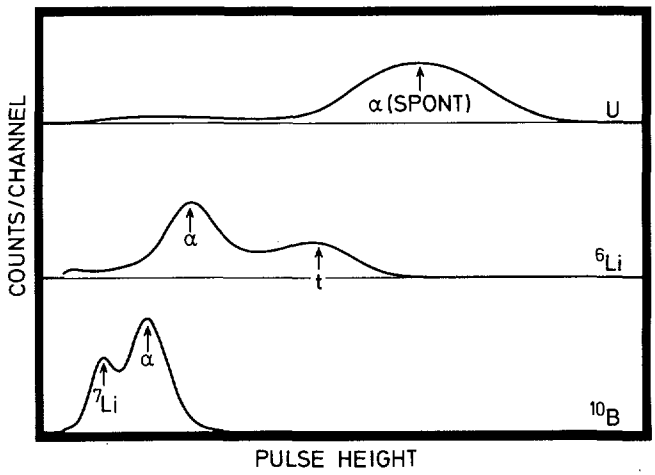

Figure 1.23 Pulse height spectra from the α-emission of ^{235}U and from the $^{6}Li(n,\alpha)$ and $^{10}B(n,\alpha)$ reactions.

The feasibility study was completed with evaluations of the compensation for anisotropies of the α emission of a hollow cylindrical sample. Secondary effects, due to the absorption of the neutron beam in the support and of the α's in the sample, should contribute less than 1 % to the error on the (n,α) ratio. Test recordings of Time Of Flight (TOF) spectra of $^{6}Li(n,\alpha)$, $^{10}B(n,\alpha)$ and $^{235}U(n,f)$ are joined to the study. Some of the runs include simultaneous recording of the pulse height spectrum of the scintillations (stability check), some include an on-line TOF-Energy conversion giving spectra according to the neutron energy.

Angular distribution of the $^6Li(n,t)^4He$ reaction

H.-H. Knitter, C. Budtz-Jørgensen, D.L. Smith*, H. Bax, R. Vogt

Triton angular distributions and forward to backward emission ratios for the $^6Li(n,t)^4He$ reaction were measured in the incident neutron energy range from 10 eV to 325 keV using pulsed white-spectrum neutrons provided by the GELINA facility. The angular distributions were measured with a new vanization detector, which offers an advantageous 2π-geometry and ns-timing capability.

The ratio of tritons emitted in the forward and in the backward hemisphere in the laboratory system was obtained in two different ways: by direct measurements of the triton energy spectra, and by calculation from the Legendre coefficients of the measured angular distributions. The agreement between both ratios forms a consistency check for the experiment. These ratios are plotted in Fig. 1.24.

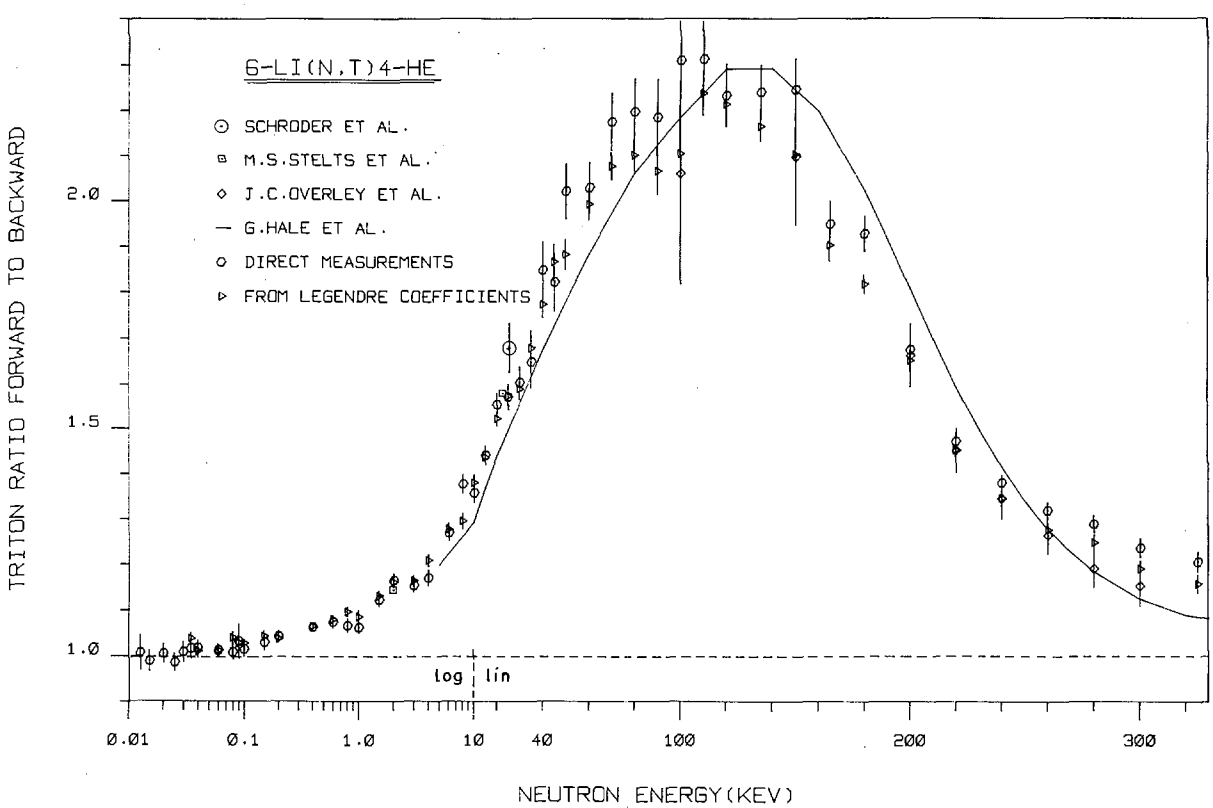

Figure 1.24 The ratio of tritons emitted in the forward and in the backward hemisphere (laboratory system).

---

* Visiting Scientist from ANL

Comparison is also made with ratios obtained from asymmetry measurements of Schröder et al. and Stelts et al. as well as with ratios obtained from angular distribution data of Overley et al.. The agreement between all the experimental data is very good. The full line in Fig. 1.24 is calculated from Hale's Legendre coefficients which are the results of an R-matrix fit. This curve shows its maximum at a somewhat higher neutron energy. Only the lowest Legendre polynomials up to L = 2 are needed to fit the angular distributions in the neutron energy range of the present experiments. With L = 3 only a marginal improvement of the fits at the highest neutron energies are possible. The relative centre-of-mass Legendre polynomial coefficients (A_1, A_2) are plotted versus the incident neutron energy in Fig. 1.25. The present experimental results are in reasonable agreement with the few existing experimental results available from literature and with the theoretical predictions of compound reaction model. They are also consistent with a direct reaction amplitude due to a deuteron exchange mechanism proposed by Weigmann and Manakos. The latter model has the advantage that it can explain the 1/v-behaviour of the $^6Li(n,t)^4He$ cross section without assuming hitherto unobserved parity states in the ^7Li-system.

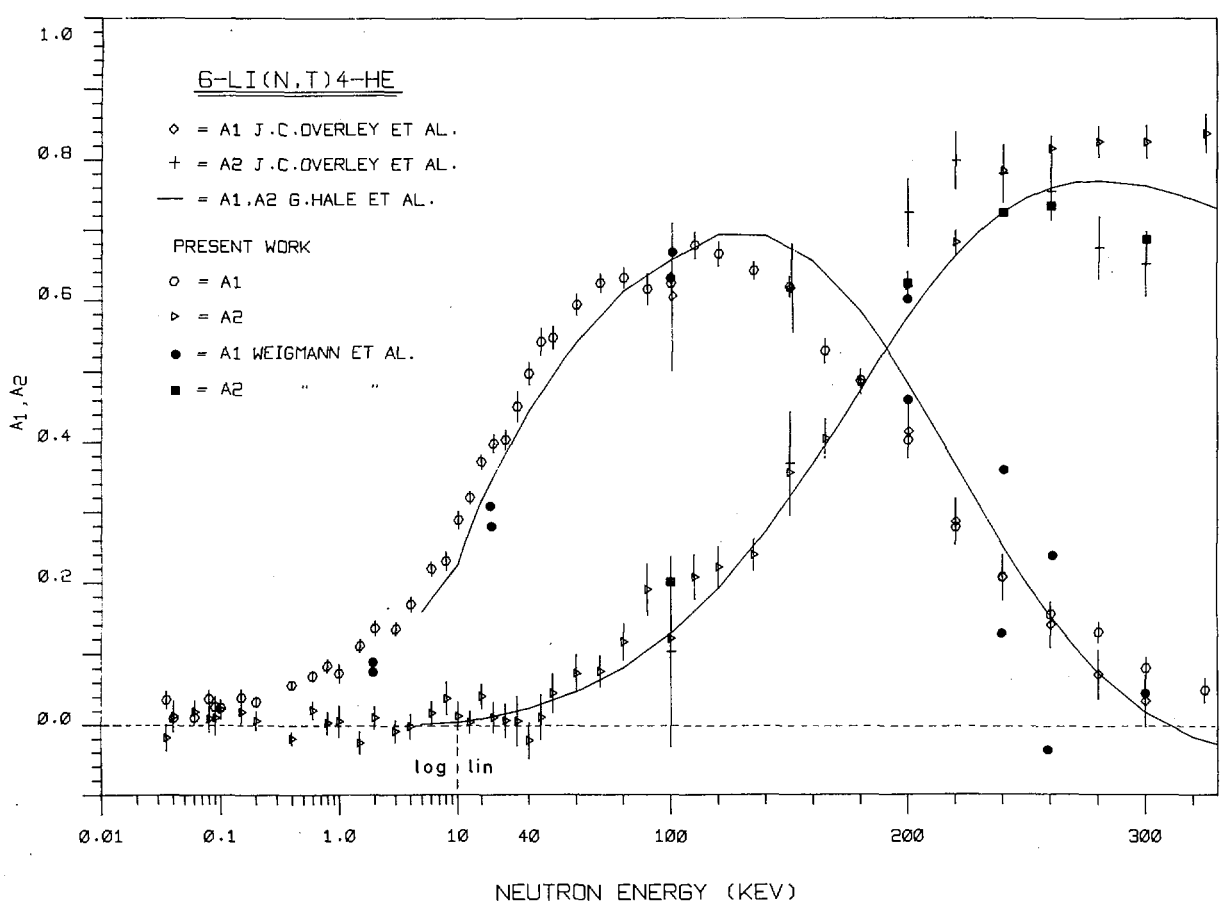

Figure 1.25 Relative Legendre polynomial coefficients (centre-of-mass system).

Average cross section ratio of $^{63}Cu(n,\alpha)$-to-$^{27}Al(n,\alpha)$

H. Liskien, D.L. Smith*, R. Widera

The neutron field produced by bombarding a thick Be-target with 7 MeV deuterons was also tested as potential "benchmark" field using a target current of 10 μA. A Cu-Al alloy sample was irradiated for about 8 hours at a distance of 8 cm in the 0° direction, from the neutron source. Thanks to the use of an alloy and the close proximity of the γ-energies involved (^{24}Na : 1368 keV, ^{60}Co : 1333 keV), a very accurate value of 0.539 $\pm$ 0.009 was obtained for the spectrum averaged cross section ratio of $^{63}Cu(n,\alpha)^{60}Co$-to-$^{27}Al(n,\alpha)^{24}Na$. This experimental value is compared with calculated values derived from differential cross section evaluation and spectrum information, and it is found to support the recent $^{63}Cu(n,\alpha)^{60}Co$ evaluation of Winkler et al. (1).

International fast neutron fluence intercomparisons

H. Liskien, R. Widera

CBNM participated in two intercomparisons running under the auspices of BIPM Sèvres. The first one, organized by CBNM, is based on $^{115}In(n,n')$ activation. Participating laboratories have to produce "quasi-monoenergetic" neutrons of 2.5, 5.0 and 14.8 MeV with known intensities and have to irradiate delivered indium samples (20 mm Ø, 5 mm thick) for a given time (5 h). After the irradiation a Ge(Li) detector has to be used to compare count rates due to the induced ^{115m}In (E_γ = 336 keV) with count rates from a delivered ^{51}Cr-source (E_γ = 320 keV).
The second intercomparison, organized by NPL Teddington, is limited to 14 MeV neutrons. Zr/Nb probes have to be irradiated by a fluence of at least $2 \cdot 10^9$ cm^{-2}. The intercomparison is based on ^{92m}Nb counting performed at NPL. Additional $^{89g+m}Zr$ counting allows to determine the average neutron energy. This is due to the fact that the $^{90}Zr(n,2n)$ cross section varies rapidly in the 14 MeV region while the $^{93}Nb(n,2n)$ cross section stays constant.

---

* Visiting Scientist from ANL

(1) G. Winkler, D.L. Smith, J.W. Meadows
Proc. International Conference on Nucl. Cross Sections for Technology, Knoxville, 1979, NBS Special Publication 594, page 199

Our measurements based on Indium activation are described in the Internal Report GE/R/VG/36/81. They are based on proton recoil counting employing a telescope counter as shown in Fig. 1.26 and have been repeated within one month to check reproducibility (0.9 - 1.2 %).

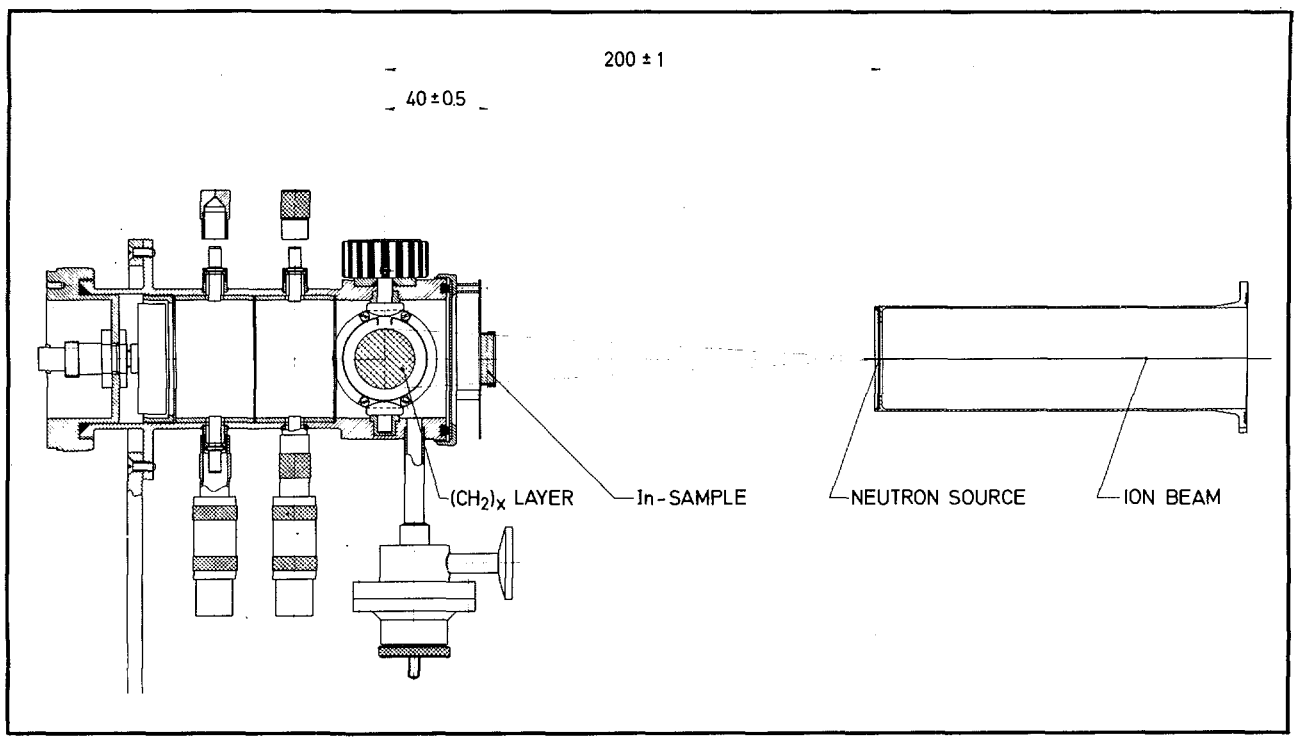

Figure 1.26 The proton recoil telescope used for fluence determination and the geometry in which the indium samples have been activated for international intercomparison.

Corrections for spurious neutrons of lower energy were determined using a calibrated TOF spectrometer with γ-discrimination based on NE-213 scintillation. The counting efficiency of the Ge(Li) detector for ^{51}Cr has been found stable within 0.1 % while the efficiency ratio for ^{51}Cr and ^{115m}In has been determined as 0.928 $\pm$ 0.002.
Irradiation of the Nb/Zr probe has been performed early November 1981. The activated probe together with the fluence as determined by us have been sent to NPL.

1.7 UNDERLYING PHYSICS

Fission fragment angular distributions and kinetic energies for $^{235}U(n,f)$ and $^{232}Th(n,f)$

C. Budtz-Jørgensen, J. Meadows*

A fission chamber employing a technique (1) developed at CBNM was investigated as a detector for simultaneous measurements of fission fragment angular distributions and kinetic energies. At the Argonne National Laboratory Fast Neutron Facility these quantities were measured for $^{235}U(n,f)$ in the incident neutron energy range from 0.15 to 10 MeV with an energy spread of $\approx \pm$ 50 keV and for $^{232}Th(n,f)$ covering the energy range from 1.5 to 1.8 MeV with an energy spread of $\pm$ 8 keV.
The evaluation of the experimental data is being made both at ANL and CBNM. The obtained angular distributions for $^{235}U(n,f)$ are in good agreement with previous data as examplified in Fig. 1.27. The anisotropies of the high resolution angular distributions measured for $^{232}Th(n,f)$ are shown in Fig. 1.28(b).

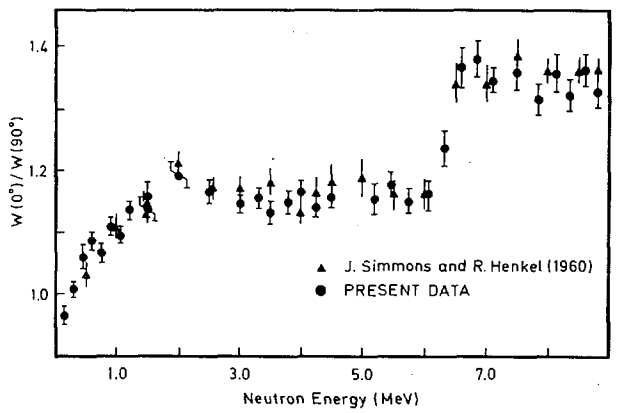

Figure 1.27 $^{235}U(n,f)$ Anisotropy.

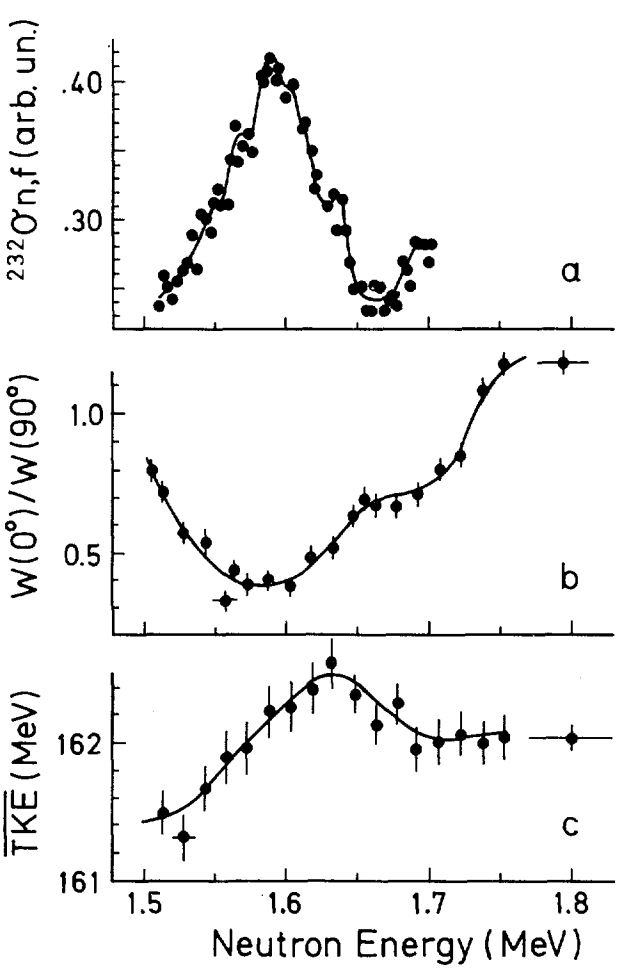

Figure 1.28 The fission process of ^{232}Th; (a) the cross section, (b) the anisotropy, (c) the average total kinetic energy released, all as function of the neutron energy.

---

* Applied Physic Division, Argonne National Laboratory, U.S.A.

(1) H.-H. Knitter, C. Budtz-Jørgensen Conf.-791022 8430, NBS 594, 1980

These distributions are important for the understanding (K-quantum number assignment) of the vibrational resonance structures observed in the ^{232}Th(n,f) cross section near threshold. The employed fission detector is well suited for fragment kinetic energy measurements since the additional angle information obliviates corrections for the variation of energy loss within the fission part produced by changing angular distributions of the fission fragments. Thus, it was demonstrated that fission fragment kinetic energies could be measured to within ≈ 100 keV.
Fig. 1.28(c) shows the measured average total kinetic energies of the ^{232}Th(n,f) fission fragments after neutron emission. A dramatic TKE change of ≈ 1 MeV is observed over a neutron energy range of only 0.2 MeV. A satisfying explanation of this behaviour has as yet not been found.

Second Chance Fission Threshold

H.-H. Knitter, C. Budtz-Jørgensen

The feature of the second-chance fission threshold allows one to obtain the height of the highest of the two barriers of the target nucleus, if the difference in the two barrier heights is larger than about 300 keV. The second chance fission cross section may be written as

$$\sigma_{n,n'f}(E) = \sigma_{n,n'} \cdot \frac{T_f}{\sum_c T_c}$$

with

$$T_f(E_n) = \int_0^\infty \frac{1/T^2 \, \epsilon \, e^{-\epsilon/T}}{1 + \exp\left[2\pi(V - E_n + \epsilon)/h\omega\right]} \, d\epsilon$$

This equation was fitted to experimental (n,n'f) cross sections. In principle three parameters must be determined by the fit. $h\omega$ describes the barrier curvature and V the threshold height. T is the temperature of the residual nucleus. The results, however, are rather insensitive with respect to $h\omega$; therefore this parameter was fixed to a value of 1.0 MeV which is commonly seen in literature. The T-values obtained by the fits agree with those measured in inelastic neutron scattering experiments. Fig. 1.29 shows the fit to data of ^{240,242,244}Pu.

Neutron capture and the doorway state

G. Rohr

This contribution has been presented as an invited paper at the International Conference on Neutron Capture Gamma Ray Spectroscopy and Related Subjects (Grenoble, Sept. 1981). It deals with a proposal for a unified capture model based on the weak coupling compound model suggested by Weisskopf. The formation of the compound state is understood as a series of collisions of two nucleons. This process is very limited with respect to the number of collisions and depends on the density of the single particle states at the Fermi surface energy and the excitation energy. The average number of particles and holes participating in the highly excited compound state is determined by means of the level density systematics. With this information the capture γ-ray emission process is interpreted mainly as a de-excitation of the compound state. The different phenomena observed in capture γ-ray spectra are caused by compound states of different hierarchy. The non-statistical effects are divided into capture in doorway resonances and capture in intermediate doorway structures. The existence of the so-called pygmy resonance observed as a structure in the γ-ray spectra for nuclei near closed shell is used to study the decoupling conditions of strong E1-transitions from the giant dipole resonance.

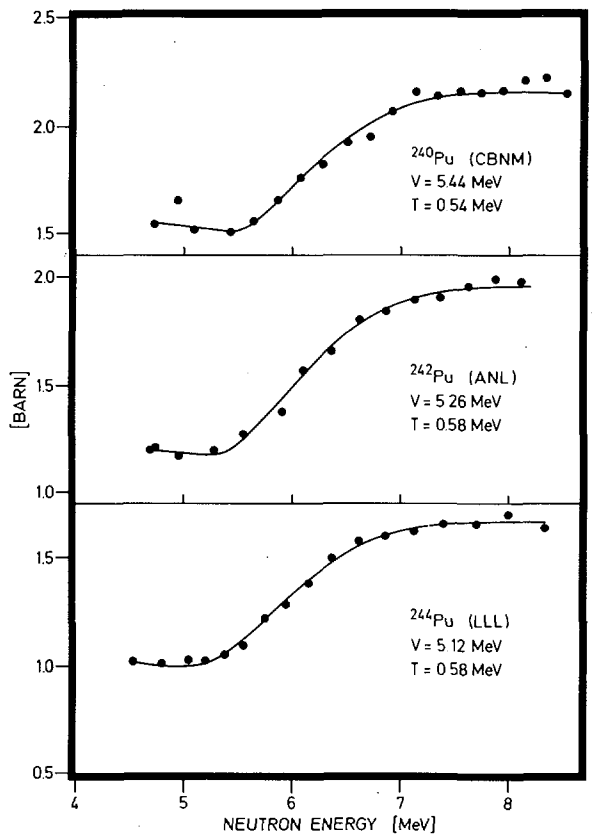

Figure 1.29 Fission cross sections of plutonium isotopes. Full lines are theoretical calculations, points are experimental data.

1.8 MAJOR RESEARCH EQUIPMENT

Electron Linear Accelerator

J.M. Salomé, R. Cools, R. Forni, F. Massardier, F. Menu, K. Meynants, P. Siméone, F. Van Reeth, J. Waelbers, C. Waller

During the period 01.11.1980 to 31.10.1981, the accelerator was operated according to the parameters given in Table 1.1.3. On the average, 4.5 neutron beams were used simultaneously for neutron measurements. Low energy electron beams, with mean currents of 50 μA at 44 MeV were produced four times for activation analysis.

Table 1.8

Operational parameters of the linear accelerator

Pulse length ns	Rep. rate Hz	Peak current A	Mean energy MeV	Time h	Time %
4 - 5	800	(6) 10 - 12	110	2830	86
16 - 20	40-100	7 - 5	100	344	10.5
1800	300	0.14	44	69	2
Miscellaneous				44	1.5

In May 1981, the operation of the Linac was interrupted for the installation of a new pre-bunching cavity and some improvements of the magnetic field between the gun and the first section. Also the optics of the gun was slightly modified to get a smaller beam diameter at high currents. Two small coils were placed at the output of the anode to maintain a very narrow beam just after the gap cathode-anode. The pre-bunching cavity is driven with up to 30 kW peak power. It should improve the efficiency of the first section. These modifications were achieved in a period of 3 weeks.

As preliminary results, a significant influence of the cavity was observed, but it was not yet possible to demonstrate completely an improved performance of the accelerator due to vacuum problems in the section 3 which lead to a destruction of an alumina window and dispersion of SF_6 in the sections and the gun. These problems were overcome. RF power from the klystrons has been increased following the setting of new circuits on the big thyratrons to divert the inverse current just after the main modulator pulses.
The pulse compression magnet is now being machined. The coils are already manufactured. At the beginning of next year the magnet will be ready for tests at the factory (without electron beam).

Automatic data taking at the Linac
C. Bastian, S. de Jonge

The ND 6660 acquisition systems at the Linac have CAMAC connections to hardware scalers, start/stop units, sample changers, etc. This allows to make elaborate cross section measurements with a minimum of human intervention. Based on software material delivered by the firm Nuclear Data Inc., a comprehensive set of measurement schemes (jobstreams) was written, tested and put into operation for transmission, capture and fission measurements. All these schemes include safety automatic transfers of the intermediate results to disk files at regular intervals. A standard set of operation keywords (START, PAUSE, CLEAR, etc.) allows a quick and fool-proof intervention. Usual experimental adjustments (e.g. changes in TOF accordion schemes or weighting functions) may be introduced without essential modifications. A user's handbook was published.

Van de Graaff accelerators

A. Crametz, P. Falque, J. Leonard, W. Schubert

During the 224 working days in 1981 - which corresponds to 1792 normal working hours - the facilities were manned 2865 hours. The break-down of this number is given below.

CN - 7 MV			KN - 3.7 MV	
accelerator running		2205		105
experiments	1945		95	
adjustments	110		10	
conditioning	150*		-	
maintenance and improvements		385		320

* not manned

The operation of the accelerators has been strongly influenced by the renewal of the target hall climatization. Running of the accelerators during day-time was excluded during several months, but by increasing night work, the operation hours were kept at a normal level. Works for the climatization have been scheduled to coincide with maintenance and improvement work whenever possible.

Repair of the CN was mainly due to (a) a leaking insulation at the power supply of a beam steerer, which led to target beam instabilities which was difficult to detect and (b) a misalignment of the drive pulley bearings in their housing which destroyed one spindle of the pulley.

A home-made ion source for the CN-accelerator had a life-time of 1290 hours. A device to measure the pulse width as described earlier was copied and installed at a second beam line. The rebuncher after the slits (with extension of the water cooling system), cables for its remote control and the 20 kW HF power amplifier have been installed. The vacuum system on the accelerator has been modified accordingly.

At the KN-accelerator the analysing magnet and its power supply were modernized by replacing the motor generator by a solid state power supply, and by replacing the corresponding magnet coils. The installation of a switching magnet and of two beam tubes ($\pm$ 15°) after the magnet has been performed. This accelerator is now also equipped with a new nuclear magnetic resonance equipment.

2. NON-NEUTRON NUCLEAR DATA

2.1 DECAY STUDIES

Half lives of ^{57}Co, ^{103}Ru, $^{103}Rh^m$, ^{103}Pd, ^{109}Cd

R. Vaninbroukx, G. Grosse, W. Zehner

A paper has been published with the following abstract (1):

" The half lives of five radionuclides were redetermined by photon-counting techniques using NaI(Tl) and Si(Li) detectors. The results are: ^{57}Co: (271.90 ± 0.09)d, ^{103}Ru: (39.260 ± 0.020)d, $^{103}Rh^m$: (56.114 ± 0.020)m, ^{103}Pd: (16.991 ± 0.019)d, and ^{109}Cd: (461.90 ± 0.30)d. The quoted uncertainties, corresponding to a 1σ level, take into account random and systematic uncertainties."

Decay of $^{93}Nb^m$

D. Reher, R. Vaninbroukx

The measurements for the determination of the half life of $^{93}Nb^m$ have been continued using Si(Li) detectors. Four sources prepared from two different samples have been measured 26 times over a period of 4.4 years.
The mean value of the preliminary result is: $T_{1/2}$ = (16.1 ± 0.6)a. This value agrees excellently with the value of (16.1 ± 0.4)a communicated by R. Lloret (2).
A paper on the determination of internal conversion electron data has been submitted for publication with the following abstract (3):

" The internal conversion ratios and the internal conversion probabilities of the 30.75 keV transition in the $^{93}Nb^m$ decay were determined to be K/LM+ = 0.19 ± 0.02, L/MN+ = 3.8 ± 0.4, K/L = 0.24 ± 0.03, κ_K = 0.17 ± 0.02, κ_{L+} = 0.85 ± 0.06, κ_L = 0.67 ± 0.09, and κ_{MN+} = 0.18 ± 0.03. Comparison of the experimental results with theoretical predictions shows good agreement."

---

(1) R. Vaninbroukx, G. Grosse, W. Zehner
New Determination of the Half-lives of ^{57}Co, ^{103}Ru, $^{103}Rh^m$, ^{103}Pd, and ^{109}Cd. Int. J. Appl. Radiat. Isot. 32, 589 (1981)

(2) R. Lloret (CEN Grenoble), Private Communication, January 1980

(3) D. Reher
The Internal Conversion in $^{93}Nb^m$, submitted to Int. J. Appl. Radiat. Isot.

Decay of $^{103}Rh^m$

R. Vaninbroukx, W. Zehner

A technical note has been submitted for publication [1]. It describes the determination of the KX-ray emission probability in the decay of $^{103}Rh^m$. The following value was found: $P_{KX} = (8.43 \pm 0.13)\ 10^{-2}$.

Half life of excited nuclear levels

H.H. Hansen, D. Mouchel, A. Nylandsted Larsen*

A paper has been published with the following abstract [2]:

"The half life of the first excited state at 6.21 keV in ^{181}Ta has been measured using the delayed coincidence technique. Si(Li) detectors of high energy resolution and a time-to-amplitude converter were used in these experiments. Great care was taken to reduce and determine the rate of accidental events. The final result for the half life from 18 measurements was found to be $T_{1/2} = (6.05 \pm 0.12)\mu s$. This value is significantly lower than previously published ones. Possible reasons for this discrepancy are discussed".

Experiments for the determination of the half life of the first excited level at 37.2 keV in ^{121}Sb have been accomplished. A paper has been submitted for publication with the following abstract [3]:

" The half life of the first excited state at 37.1 keV in ^{121}Sb has been measured using the technique of delayed coincidences with a time-to-amplitude converter. Scintillators with fast timing properties have been used in various combinations. From 17 independent measurements a result for the half life of $T_{1/2} = (3.46 \pm 0.03)$ ns has been obtained and this is compared with previously published values."

---

* Present address: Det Fysike Institut, Århus Universitet

(1) R. Vaninbroukx, W. Zehner
Determination of the KX-ray Emission Probability
Int. J. Appl. Radiat. Isot. 32, 850 (1981)

(2) D. Mouchel, A. Nylandsted Larsen, H.H. Hansen
Half life of the 6.21 keV level in ^{181}Ta
Z. Phys. A300, 85 (1981)

(3) H.H. Hansen, D. Mouchel, A. Nylandsted Larsen
Half life of the 37.1 keV level in ^{121}Sb
Z. Phys. A in press

Decay of ^{133}Ba

H.H. Hansen, G. Grosse, D. Mouchel, R. Vaninbroukx

The half life determinations continued. Two sets of γ-ray spectra were measured with the Ge(Li) and one new set with the NaI(Tl) detector. Both types of experiments give results in good agreement. The errors are still rather high due to the relatively short observation period.
Some additional spectra of internal conversion electrons of the 80.9 and 160.6 keV transitions in ^{133}Cs had to be remeasured. Unstable and unreproducible experimental conditions led to some unexpected complications, which made these additional runs necessary. This is especially true for the recording of the electron spectra of the very low intensity 160.6 keV transition. The evaluation of the new runs is going on and the results will be incorporated into the set of values already determined before.

Decay of ^{224}Ra

G. Bortels, D. Reher, R. Vaninbroukx

A paper has been presented at the ICRM Seminar on Alpha-Spectrometry Techniques and Application, Geel, 14 October 1981. It has the following abstract:

" The emission probability for the 5.449 MeV α particles from the transition, which in the decay of ^{224}Ra populates the 241 keV level in ^{220}Rn, has been determined by α spectrometry. Sources of ^{224}Ra, produced by recoil implantation from ^{228}Th, were measured using Si-surface-barrier detectors. A value of $P_{\alpha_1} = 0.0506 \pm 0.0004$ (1σ) is obtained; the quoted uncertainty includes random and systematic components. The result is confirmed by independent γ-spectrometric measurements using an intrinsic Ge detector."

Gamma-ray emission probabilities in the decay of the daughters of ^{228}Th and ^{232}U

R. Vaninbroukx, H.H. Hansen

For accurate mass determinations of uranium samples by α counting techniques, ^{232}U contents of about 0.1 ppb should be detectable. Its detection limit by α-particle spectrometry is about 30 ppb. Using γ-ray spectrometry concentrations of 0.1 ppb can be determined with the required accuracy, if the γ-ray emission probabilities of the ^{232}U daughters, ^{228}Th, ^{224}Ra etc. were

known well enough. This is not the case. The knowledge of these emission probabilities is also of interest for the determination of natural Th in environmental samples.

For the determination of these emission probabilities sources were made from ^{228}Th solutions. In aged uranium samples the ^{228}Th is in equilibrium with ^{232}U but for the preparation of the sources special care had to be taken in order to prevent the escape of Rn from the sources; otherwise the equilibrium between all daughter nuclides is not guaranteed. The disintegration rates N_0 of the sources were determined relative to other ^{228}Th sources using a 3" x 3" NaI(Tℓ) detector. The reference sources were prepared from a standardized ^{228}Th solution obtained from TRC, Amersham. This solution was also standardized at CBNM using a calibrated Ge(Li) detector by observing the count rates under the 583 keV peak, for which the emission probability is rather well known. For the determination of the γ-ray emission rates, N_γ, two calibrated detectors were used: the Ge(Li) detector mentioned above and a small high-purity Ge detector. For the efficiency calibration of the detectors in function of the γ-ray energies, reference sources prepared by deposition of weighed fractions of accurately standardized solutions of suitable radionuclides were used. The γ-ray emission probabilities P_γ are obtained by dividing N_γ by N_0. The preliminary results are given in Table 2.1. The quoted uncertainties, corresponding to a 1σ level, take into account random and systematic errors.

Table 2.1

Gamma-ray emission probabilities of ^{228}Th daughters

Energy E	Emission probabilities P_γ		
keV	Ge(Li)	HP-Ge	Mean
238.6	0.486 ± 0.009	0.440 ± 0.006	0.440 ± 0.006
241.0		0.0407 ± 0.0009	0.0407 ± 0.0009
277.4	0.0224 ± 0.0006	0.0231 ± 0.0004	0.0229 ± 0.0004
300.1	0.0325 ± 0.0008	0.0323 ± 0.0006	0.0324 ± 0.0006
510.8	0.0848 ± 0.0017	0.0820 ± 0.0016	0.083 ± 0.002
583.1	(0.3083 ± 0.0072)*	0.308 ± 0.006	0.308 ± 0.006
727.2	0.0707 ± 0.0021	-	0.071 ± 0.002

* Used partly as basis for the determination of the disintegration rates of the sources

Gamma-ray emission of ^{235}U and ^{231}Th

R. Vaninbroukx, B. Denecke

The present knowledge of the γ-ray emission probabilities in the decay of ^{235}U and its radioactive daughter ^{231}Th is unsatisfactory. The accuracy required for non-destructive analysis of fuel materials is $\pm$ 1 % while the achieved accuracy is $\pm$ 10 % (1). The emission probabilities for the most prominent γ transitions in the energy range between 25 and 206 keV accompanying the decay of ^{235}U and ^{231}Th, - generally in secular equilibrium with its parent ^{235}U -, were redetermined.
Twenty sources were prepared from three different uranium materials. Some details about the materials used and the definition of the ^{235}U content of the sources are given in Table 2.2.

Table 2.2

Materials used and ^{235}U determination

Material	Number of sources	^{235}U content			Activity ratio R	
		atom %	mg per source	method of determination	$\frac{I_\alpha(^{235}U)}{I_\alpha(total)}$	method of determination
U-Al alloy	6	93.22	1.5 - 25	Isotope dilution	-	-
Uranium fluoride	3	99.47	0.1 - 0.6	α counting	0.1690 $\pm$ 0.0017	Isotope analysis
Uranyl acetate	11	99.97	0.1 - 1.0	α counting	0.9716 $\pm$ 0.0010	α-particle spectrometry

For the determination of the ^{235}U disintegration rates of the sources two different methods were applied: mass spectrometric isotope dilution and α counting. The ^{231}Th disintegration rates are equal to the ^{235}U disintegration rates because they are in secular equilibrium.
For the U-Al alloy the number N of ^{235}U atoms for each of the sources was determined by mass spectrometric isotope dilution. For that purpose, the sources, after the measurement of the γ-emission rates, were spiked with a

(1) A.L. Nichols
"Transactinium Nuclear Data - 1979",
IAEA-TECDOC-232, IAEA, Vienna (1980) p. 67

well known amount of ^{233}U and dissolved. The uranium was then separated from the aluminium and the ratio $^{235}U/^{233}U$ was measured. The uncertainty of the ^{235}U determination was estimated as $\pm$ 0.5 %. The ^{235}U disintegration rate has been calculated using the half-life value recommended [1].
For uranium fluoride and uranyl acetate the ^{235}U disintegration rates were determined by α counting under a well defined low-geometry solid angle.
For the uranium fluoride samples, the corrections for the contribution from other uranium isotopes to the α count rates were calculated from the isotopic composition as determined by mass spectrometry and the decay constants derived from the recommended half lives. For the uranyl acetate samples these corrections were determined by α-particle spectrometry. The values of these corrections for both materials, expressed as the activity ratio R of the ^{235}U α activity to the total α activity are given in Table 2.1. The overall uncertainty on the ^{235}U disintegration rates becomes 0.6 % for U-Al alloy, $\pm$ 1.1 % for uranium fluoride and $\pm$ 0.7 % for uranyl acetate. All uncertainties correspond to a 1σ confidence level and include random and systematic uncertainties.
The γ-ray emission rates of all the sources were determined using three calibrated photon detectors: a Si(Li) detector with an area of 3 cm^2 and a thickness of 3 mm and two high purity Ge detectors, one with an area of 1 cm^2 and a thickness of 8 mm (detector GE-I), and one with an area of 3 cm^2 and a thickness of 10 mm (detector GE-II). The Si(Li) detector was used to measure the γ rays of 25.65 keV and 84.16 keV following the decay of ^{231}Th, while the two Ge detectors were used for the two γ rays mentioned and for those of 143.8, 163.4, 185.7, and 205.3 keV accompanying the decay of ^{235}U. The solid angles of the detector systems were about 0.2 sr for the Si(Li) detector, 0.1 sr for GE-I, and 1 sr for GE-II. A typical ^{235}U - ^{231}Th γ-ray spectrum in the energy range concerned here is shown in Fig. 2.1.
Prior to the ^{235}U - ^{231}Th measurements the detectors were calibrated for all types of sources used.
The mean results for the γ-ray emission probabilities, obtained from the measurements on all sources using the three detectors, for the different materials are given in Table 2.3. The last column of this table gives the weighted mean values; they are our final values.

---

(1) A. Lorenz, Ed.
INDC(NDS)-121/NE (1980)

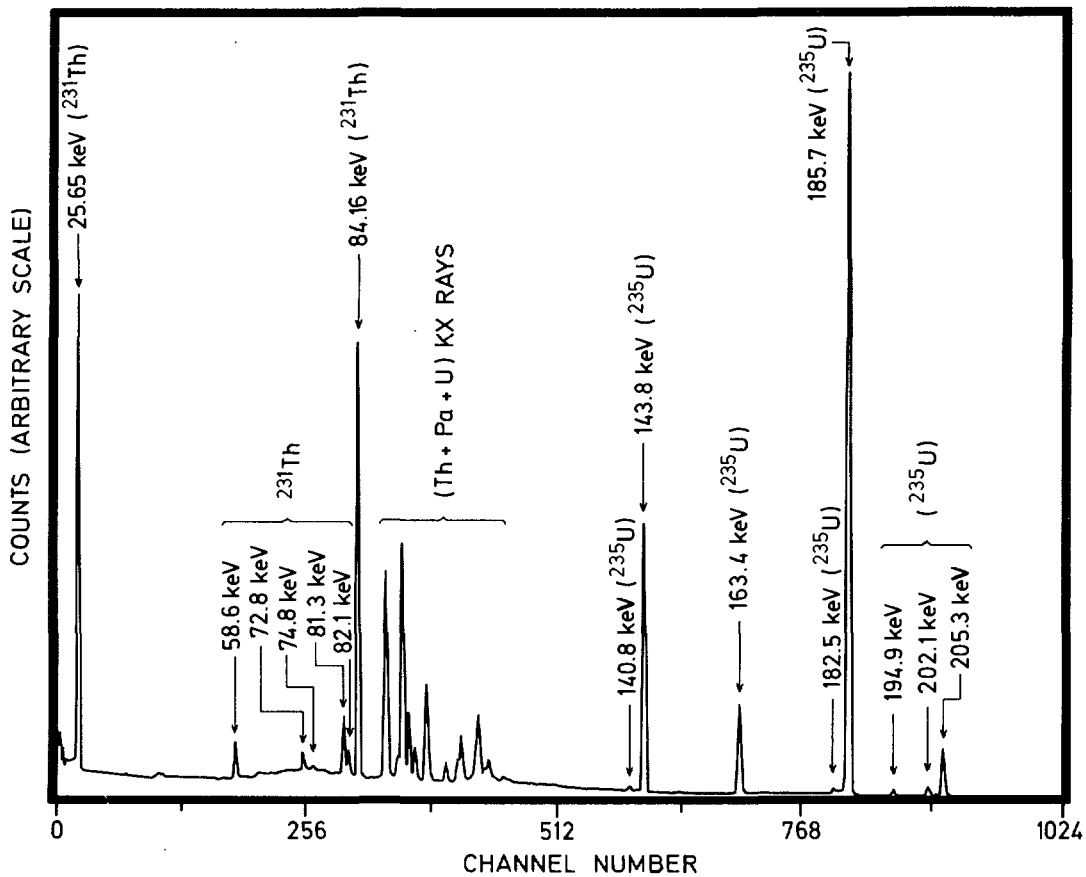

Figure 2.1 ^{235}U-^{231}Th γ-ray spectrum (Detector GE-I)

Table 2.3

Results of the γ-ray emission probability determinations

Energy (keV)	Emission probability P_γ			
	U-Al Alloy	Uranium fluoride	Uranium acetate	Final value
25.65	0.1445 ± 0.0035	0.1444 ± 0.0030	0.1453 ± 0.0028	0.145 ± 0.003
84.16	0.0666 ± 0.0020	0.0652 ± 0.0026	0.0626 ± 0.0034	0.066 ± 0.003
143.8	0.1090 ± 0.0021	0.1086 ± 0.0024	0.1084 ± 0.0023	0.109 ± 0.002
163.4	0.0502 ± 0.0011	0.0488 ± 0.0015	0.0496 ± 0.0012	0.050 ± 0.001
185.7	0.5780 ± 0.0085	0.5707 ± 0.0098	0.5755 ± 0.0088	0.575 ± 0.009
205.3	0.0494 ± 0.0015	0.0501 ± 0.0020	0.0515 ± 0.0015	0.050 ± 0.002

Our results for the 185.7 keV ray, the most intense one and often considered as a "reference" γ ray, is 6.5 % higher than the previously adopted value based on a few very old measurements [1]. The ratios of the emission probabilities of the other γ rays to that of the "reference" ray are in fairly good agreement with recent evaluated values [2,3]. The project is finished and the results [4] were presented at the 5th Symposium on X- and Gamma-Ray Sources and Applications, Ann Arbor, June 10-12, 1981. The proceedings of this conference will be published in Nuclear Instrument and Methods.

Half life of ^{241}Pu

P. De Bièvre, M. Gallet, R. Werz

The determination of the half life of ^{241}Pu by direct decay measurements using mass-spectrometric methods has been continued. Samples of Pu material (ORNL 210A, Harwell 94/241/10 and "Wilkins") were followed by measurement of the ^{241}Pu/^{240}Pu ratio and also of the (^{241}Pu/^{240}Pu)/(^{240}Pu/^{239}Pu) ratio over a period of 6 years. During that period about 29 % of the ^{241}Pu atoms decayed. Values for the half life were derived from least-squares fits (Fig. 2.2a). The deviation of the data points from the fitted values is less than 0.06 % (Fig. 2.2b).

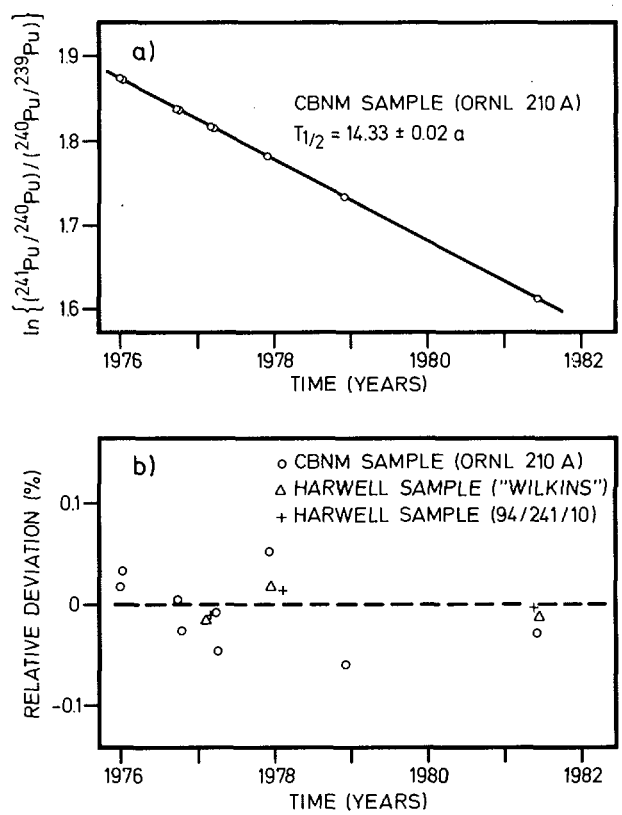

Figure 2.2 Determination of ^{241}Pu half life. a) least-squares fit of half-life measurements. b) relative deviation of the results from the fitted values.

(1) E.K. Hyde, I. Perlman, G.T. Seaborg
"The Nuclear Properties of the Heavy Elements, Vol.II: Detailed Radioactive Properties, Prentice Hall, Inc., Englewood Cliffs, N.J. (1964)

(2) M.R. Schmorak
Nucl. Data Sheets 21 (1977) 91

(3) C.M. Lederer, V.S. Shirley, Eds., "Table of Isotopes, 7th edition", John Wiley and Sons, Inc. New York (1978)

(4) R. Vaninbroukx, B. Denecke
Determination of the Gamma-Ray Emission Probabilities in the Decay of ^{235}U and ^{231}Th, Nucl. Instr. Meth. in press

Preliminary results of the ^{241}Pu half life (in years) are listed in Table 2.4. The results are further evaluated and will be published.

Table 2.4

Preliminary results of ^{241}Pu half life (in years)
Uncertainties are given in standard deviations

Method	CBNM sample ORNL 210A	Harwell samples	
		"Wilkins"	94/241/10
$^{241}Pu/^{240}Pu$	14.34 ± 0.03	14.32 ± 0.03	14.32 ± 0.03
$\frac{^{241}Pu/^{240}Pu}{^{240}Pu/^{239}Pu}$	14.33 ± 0.02	14.35 ± 0.02	14.33 ± 0.01

2.2 COMPILATIONS AND EVALUATIONS

Internal conversion data

H.H. Hansen

The compilation of experimental values of internal conversion data for nuclei with $Z \leqslant 60$ has been published (1) with the following abstract:

" A compilation of experimental values of internal conversion coefficients and ratios is presented. Results quoted with an error and published later than November 1965 and prior to December 1978 have been retained. Separate tables have been prepared for results from studies on radioactive nuclides, from nuclear reaction experiments, from measurements on E0 transitions, and from studies in different chemical environments. The tables include information on the origin of the isotope, transition energies, spin and parity of initial and final levels, experimental technique used, and literature references."

(1) H.H. Hansen
Compilation of experimental values of internal conversion coefficients and ratios for nuclei with $Z \leqslant 60$, Physik Daten/Physics Data 17-1 (1981).

The evaluation of total and K-shell internal conversion coefficients for the transitions of 14.4, 122.1 and 136.5 keV in ^{57}Fe have almost been accomplished. Similar work on internal conversion data on the 279.2 keV transition in ^{203}Tl and on the 411.8 keV one in ^{198}Hg are in progress.

Directory of certified radioactive reference sources

W. Bambynek, G. Grosse

On request of the International Atomic Energy Agency, Vienna, an International Directory of Certified Radioactive Sources has been compiled and stored on disk for retrieval by computer. It lists the products given in the catalogues of 16 suppliers. These products are divided into four groups: radioactive solutions, radioactive gases, solid sources, and sources for liquid scintillation counting. The data have been written on a magnetic tape and will be sent to the IAEA.

2.3 UNDERLYING PHYSICS

Internal conversion ratios in the decay of ^{152}Eu

H.H. Hansen, D. Mouchel

The evaluation of a series of internal conversion electron spectra has been finished. The results have been summarized in an internal report with the following abstract [1]:

" Measurements have been made with a magnetic β spectrometer in order to determine the internal conversion ratios R = K/LM+ for two pure E2 transitions of 244.7 and 344.3 keV in the decay of ^{152}Eu. The results from 7 experimental runs for each transition are respectively R = 2.92 ± 0.05 and R = 3.43 ± 0.05. A comparison has been made with previously published results as well as with theoretical values deduced for pure E2 multipolarity from the most recent tabulations of internal conversion coefficients."

---

(1) H.H. Hansen, D. Mouchel
K/LM+ Internal Conversion Ratios for Pure E2 Transitions in the Decay of ^{152}Eu, CBNM/RN/25/81

Scattering and absorption of α particles

B. Denecke

A study is in progress to understand quantitatively the distribution effect of recoiling atoms, and their subsequent decay, on the measurement of α-particle spectra with Si detectors. In particular the case of the decay of ^{228}Th is under investigation. Two detectors with respectively a 20 and 40 μg/cm^2 Au layer were considered. The mean range of the implants on ^{224}Ra in Au is 34 μg/cm^2 with 40 % range straggling. The initial distribution of the ^{224}Ra atoms has a maximum concentration at the Au surface extending into the Si material. After each subsequent decay of ^{224}Ra and its α-decaying daughters the local distributions of the decaying nuclides are changed. Deeper migration into the Si material and escape from the Au surface take place.

Spectra from the two Si detectors will show an α peak and a sum peak of the α energy and the recoil energy which are dissipated in the Si. Both peaks are distorted by energy absorption in the Au and energy from the Si escape. Consequently, corrections have to be employed for the position shifts of the observed peak maxima.

In order to obtain these corrections the detection process was simulated by a Monte Carlo programme. The density distributions of the subsequent radioactive nuclides were generated by folding the initial distribution with the recoil range and straggling functions (Fig. 2.3a). In these simulations the α-energy absorption in the Au layer and the recoil-energy absorption in the Si were calculated using (a) the generated nuclide distributions

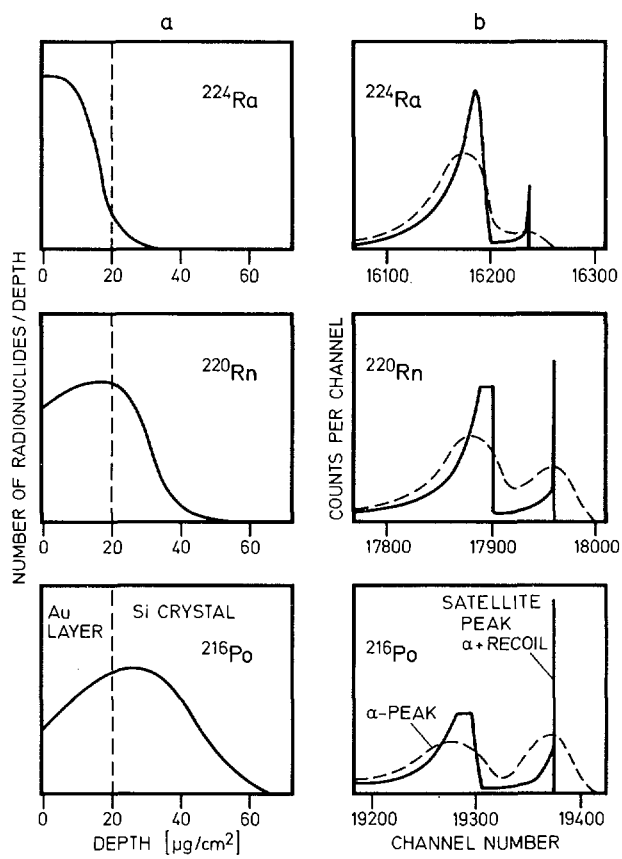

Figure 2.3 a) Depth profile of three ^{224}Ra decay chain members in a Si-SB detector. b) Simulated spectra showing α peaks and satellite peaks before (fulle line) and after folding (dotted line) as described in the text.

and (b) the integrated stopping-power functions for α particles [1] and heavy ions [2].
Finally the spectra (Fig. 2.3b) were folded with the detector response function. The shift of the peak maximum towards lower energies, found in this way, was used as correction in the determination of the fraction of heavy-ion energy absorption due to electronic stopping in Si.

2.4 IMPROVEMENT OF MEASUREMENTS AND SOURCE PREPARATION TECHNIQUES

Comparison of activity measurements of a ^{133}Ba solution

D. Reher, E. Celen, R. Vaninbroukx

This comparison was organized by the Bureau International des Poids et Mesures (BIPM) on behalf of Section II (Mesures des Radionucléides) of the Comité Consultatif pour les Etalons de Mesures des Rayonnements Ionisants. The participating laboratories in this mini-comparison were AECL, BIPM, CBNM, LMRI, OMH and PTB. The nuclide ^{133}Ba was chosen for metrological and practical reasons. It is of great importance for the efficiency calibration of semi-conductor spectrometers and is often used as a mock-standard for the short-lived ^{131}I in medical and environmental applications. The objectives of such a mini-comparison are to test the standardization procedure and to identify possible difficulties which have to be avoided in a large scale comparison. Each laboratory received an ampoule containing about 1 MBq ^{133}Ba dissolved in 1 ml 1 M HCl. The activity has been determined by the 4π(AX)-γ coincidence method using the efficiency extrapolation technique. Due to problems with the first measurements CBNM received a second ampoule.
The results obtained were 1130.5 $\pm$ 1.8 Bq/mg for the first ampoule and 1115.6 $\pm$ 1.7 Bq/mg for the second one. Other participants in the comparison reported similar problems. A detailed analysis of the results at CBNM showed that there were evidently difficulties of a chemical nature. Adsorptions, presumably on the ampoule walls, of up to 0.6 % were reported.

---

(1) J.F. Ziegler
Helium Stopping Powers and Ranges in all Elemental Matter,
(Pergamon Press, London, 1978)

(2) H. Oetzmann, A. Feuerstein, H. Graham, S. Kalbitzer
Range Parameters of Heavy Ions in Amorphous Targets at LSS Energies of $0.0006 \leqslant \epsilon \leqslant 0.3$, Phys. Letters 55A, 170 (1975)

A second mini-comparison was organized. Again, AECL, BIPM, CBNM, LMRI, OMH and PTB are participating. The solution for this comparison was distributed by PTB. Each participant received one ampoule containing about 3.6 ml of $^{133}BaCl_2$ solution. Adsorption tests, impurity checks, source preparation, are in progress.

Low energy X-ray standards

A. Kacperek*, B. Denecke, D. Reher, W. Bambynek

A paper has been published with the following abstract (1):

" The standardization of X-ray sources for the calibration of Si(Li) detectors at energies below 4.5 keV is described. An Al KX-ray emission source is taken as an example. The effect of source anisotropy is measured for different solid angles > 10 msr and for non-normal source emission. An accuracy of better than 3 % is achieved".

Preparation and characterization of thin $^{93}Nb^m$ sources

D. Reher, W. Oldenhof, I.V. Mitchell

For the preparation of thin, homogeneous and laterally uniform sources of $^{93}Nb^m$ several techniques were employed, i.e. drop deposition, drop deposition with freeze drying, electrostatic spraying and focused ion-beam sputtering. The characteristics of these sources were determined using four different non-destructive methods: Rutherford backscattering (RBS), particle-induced X ray emission (PIXE), electron spectrometry and autoradiography. RBS and PIXE show that focused ion-beam sputtering gives the thinnest and purest layers; while the drop deposited ones contain chemical impurities. Qualitative information for the self absorption of electrons in the deposits was obtained from electron spectrometry. It was found that layers produced by focused ion-beam sputtering showed the least self absorption. Electrostatic spraying gave also good results.

---

* Bursary of the European Community

(1) A. Kacperek, B. Denecke, D. Reher, W. Bambynek
The Standardization of X-Ray Sources below 4 keV,
Nucl. Inst. Meth. in press

From several sources, prepared by the different methods, auto-radiographs have been made and scanned using an optodensitometer. The light absorption curves, shown in Fig. 2.4, are related to the amount of radiation emitted per area from the sources. From these curves it is evident that focused ion beam sputtering produces the most homogeneous and laterally uniform sources. We conclude that the focused ion beam sputtering technique, applied for the preparation of very thin and laterally uniform radioactive sources, is superior to many other methods, especially when refractory materials have to be deposited. The non-destructive techniques used in the characterization of the produced layers have shown to be very useful.
A paper [1] was presented at the 5th Symposium on X- and Gamma-Ray Sources and Applications, Ann Arbor, June 10-12, 1981.

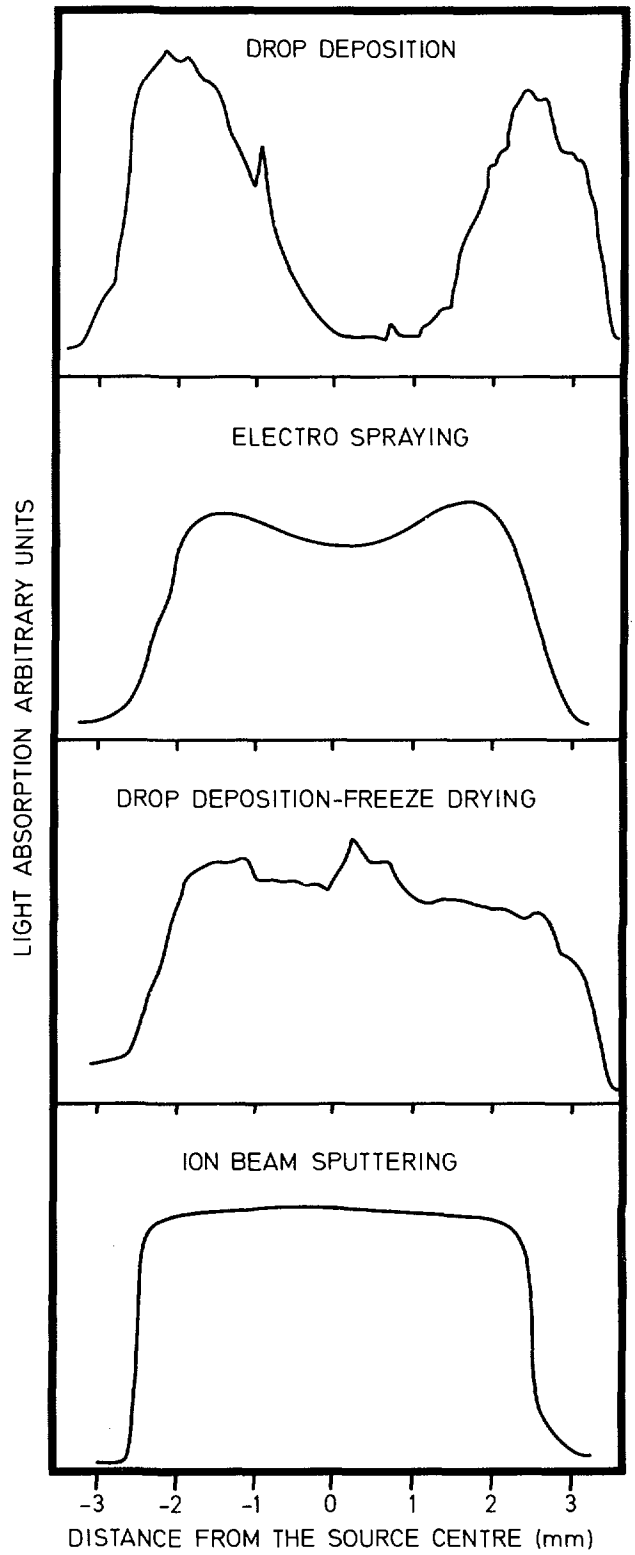

Figure 2.4 Light absorption curves from auto-radiographies of $^{93}Nb^{m}$ sources, prepared by different techniques.

(1) D. Reher, I.V. Mitchell, W. Oldenhof
The Preparation and Characterization of Radioactive Sources of Refractory Metals for Low-Energy X-Ray and Electron Spectrometry, Nucl. Inst. Meth. in press

Source preparation

W. Oldenhof, W. Zehner

Two installations are under construction to prepare thin sources of small amounts (μg) of radioactive material.
The principle of the first technique is the evaporation of the material under vacuum (10^{-6} torr) from a Ta crucible in the form of a chimney (inner diameter 0.2 mm, outer diameter 1.5 mm, length 12 mm). This can be heated up to 2000°C by electron bombardment from a tungsten filament. With this technique a yield of 30 to 40 % can be obtained depending on the distance between source and target. The apparatus is placed in a glovebox.
The principle of the second technique is the repeated evaporation of the material under vacuum (10^{-7} torr) during a short time (some ms). In this way heating of the target material (which usually is a thin metallized plastic foil), is kept low. Also this apparatus is built up in a glove box.
Various techniques were used for the preparation of about 150 radioactive sources (^{51}Cr, ^{55}Fe, ^{88}Y, ^{93}Nb^{m}, ^{109}Cd, ^{121}Sn^{m}, ^{133}Ba, ^{181}Hf, ^{228}Th, ^{234}U, ^{241}Am) on Vyns, Formvar and carbon foils. About 450 foils (Vyns, Formvar, carbon) were made.

Radionuclides group data acquisition system

D. Reher, B. Idzerda

The second phase of the installation of the Radionuclides Group Data Acquisition System, RNDAS, is terminated. Three autonomous intelligent (μP 6800) CAMAC systems (Fig. 2.5) control two experiments each. This includes the start, stop, read-out and reset of scalers and multichannel analyzers and the steering of stepping motors. The course of the measurements is controlled through commands from the terminal keyboard. The current state of an experiment is continuously displayed on the terminal screen and a logging of events is recorded on a TTY printer. The measured data are collected on floppy disks which can be read by the PDP 11/34 computer system. The software for the data acquisition and control of the experiments has been written to 95 % in an advanced BASIC language allowing CAMAC calls. The systems allow off-line editing and development of programmes in BASIC, CAMACRO and assembler.

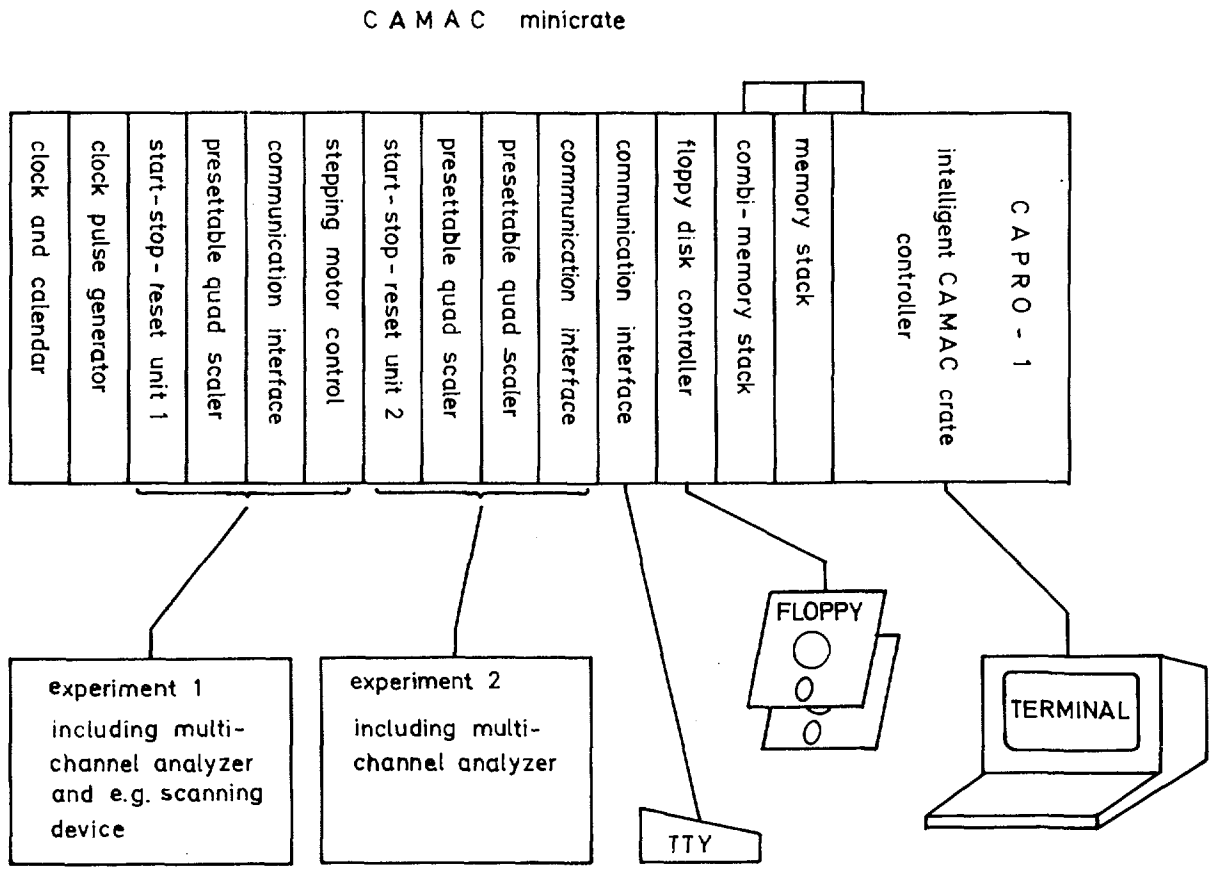

Figure 2.5 Autonomous intelligent CAMAC system.

LIST OF CBNM PUBLICATIONS

NUCLEAR DATA

1. NEUTRON DATA

Publications in periodicals

- A. EMSALLEM, M. ASGHAR, C. WAGEMANS, H. WEIGMANN
  Study of Neutron Induced Charged Particle Reactions on ^{40}K:
  Part I - Thermal Neutrons .
  Nuclear Physics A 368, 108-116 (1981).

- H. WEIGMANN, C. WAGEMANS, A. EMSALLEM, M. ASGHAR
  idem: Part II - Resonance Neutrons .
  Nuclear Physics A 368, 117-134 (1981).

- E. ALLAERT, C. WAGEMANS, G. WEGENER-PENNING, A.J. DERUYTTER, R. BARTHELEMY
  Energy and Mass Distributions for $^{241}Pu(n_{th},f)$, $^{242}Pu(s,f)$ and $^{244}Pu(s,f)$ fragments .
  Nuclear Physics, to be published.

- C.R. JUNGMANN, H. WEIGMANN, L. MEWISSEN, F. POORTMANS, E. CORNELIS, J. THEOBALD
  Resonance structure of ^{32}S=n from transmission and differential scattering experiments .
  Nuclear Physics, to be published.

- J.M. SALOME, R. FORNI
  Measurement of Microbunch Energy Spectra on an S-band electron Linac.
  I.E.E.E. Transactions on Nuclear Science, Vol. NS-28, 81

- E. ALLAERT, C. WAGEMANS, G. WEGENER-PENNING, A.J. DERUYTTER
  "Vergelijkende studie van de spontane fissie van ^{242}Pu en de door thermische neutronen geïnduceerde fissie van ^{241}Pu".
  Samenvattingen van de Mededelingen van de Algemene Wetenschappelijke Vergadering van de B.N.V., Leuven, 1981, p. N.P.-3.

- H. LISKIEN, A. PAULSEN
  Determination of $^{7}Li(n,t)$ Cross Sections between 6 and 10 MeV.
  Annals of Nuclear Energy 8, 423 (1981).

- A. PAULSEN, H. LISKIEN, F. ARNOTTE, R. WIDERA
  Measurement of (n,α) Cross Sections of Chromium, Iron and Nickel in the 5-10 MeV Neutron Energy Range.
  Nucl. Science and Engineering 78, 377 (1981).

- C. BUDTZ-JØRGENSEN, H.-H. KNITTER
  Neutron-Induced Fission Cross Section of Plutonium-240 in the Energy Range from 10 keV to 10 MeV.
  Nucl. Science and Engineering 79, 380 (1981).

- S.M. QAIM, R. WÖLFLE, H. LISKIEN
  Excitation Functions of (n,t) reactions on ^{27}Al, ^{59}Co, ^{93}Nb.
  Physical Review C25, 203 (1982).

Conference papers

- H.-H. KNITTER, C. BUDTZ-JØRGENSEN, D.L. SMITH
  Measurement of Triton Angular Distributions for ^{6}Li(n,t)^{4}He.
  Verhandlungen der DPG 4, 675 (1981).

- C. BUDTZ-JØRGENSEN, J. MEADOWS
  Angular Distribution and Total Kinetic Energy for ^{232}Th(n,f).
  Proc. of "Nuclear Fission and Related Collective Phenomena and Properties of Heavy Nuclei", Bad Honnef (1981) to be published in "Lecture Notes in Physics", Springer Verlag, Edited by P. David.

- A. BRUSEGAN, F. CORVI, G. ROHR, R. SHELLEY, T. VAN DER VEEN
  Resonance Interference in ^{54}Fe s-wave Capture.
  4th Int. Symp. on Neutron Capture Gamma Ray Spectroscopy and Related Topics, Grenoble, 7-11 Sept. 1981.

- M.S. MOORE, F. CORVI, L. MEWISSEN, F. POORTMANS
  Parity Assignment of the Pronounced Structure in Radiative Capture of Neutrons by ^{238}U below 100 keV.
  ibid.

- B.J. ALLEN, A. BRUSEGAN, R. SHELLEY, T. VAN DER VEEN, G. VANPRAET
  Search for Valence Effects in p-wave Capture in ^{88}Sr.
  ibid.

- A. BRUSEGAN, B.J. ALLEN, F. CORVI, G. ROHR
  Failure of Valence Neutron Capture in ^{96}Zr.
  ibid.

- C. WAGEMANS, H. WEIGMANN
  Study of (n,alpha) and (n,p) Reactions with Resonance Neutrons.
  ibid.

- H. WEIGMANN
  Review of ^{240}Pu and ^{242}Pu Resolved Resonance Parameters.
  IAEA Consultants Meeting on U and Pu Isotope Resonance Parameters Vienna, 28 Sept. - 2 October 1981.

- F. POORTMANS, E. CORNELIS, L. MEWISSEN, G. ROHR, R. SHELLEY, T. VAN DER VEEN, G. VANPRAET, H. WEIGMANN
  Review of U-238 Resolved Resonance Parameters obtained at CBNM Geel.
  ibid.

- H. WEIGMANN
  The Influence of Intermediate Structure on Average Physics Fission Cross Sections.
  Intern. Symp. on "Nuclear Fission and Related Collective Phenomena and Properties of Heavy Nuclei",
  Inst. f. Strahlen- u. Kernphysik der Universität Bonn,
  Bad Honnef, 26-29 October 1981

- H.-H. KNITTER, C. BUDTZ-JØRGENSEN, H. WEIGMANN
  New Results on the Neutron-Induced Fission Cross Sections of 238 and 240 Plutonium.
  ibid.

Reports

- H.-H. KNITTER, C. BUDTZ-JØRGENSEN, D.L. SMITH
  Neutron-Induced Fission Cross Section of ^{238}Pu in the Energy Range from 150 keV to 10 MeV.
  Internal Report CBNM/VG/35/81.

- H. LISKIEN, R. WIDERA
  CBNM Participation in an International Fast Neutron Fluence Intercomparison based on Indium Activation.
  Internal Report GE/R/VG/36/81.

- C. BUDTZ-JØRGENSEN, P.T. GUENTHER, A.B. SMITH, J.F. WHALEN
  Fast-Neutron Total and Scattering Cross Sections of ^{58}Ni.
  ANL/NDM Report 61 (1981).

2. NON-NEUTRON DATA

Publications in periodicals

- D. MOUCHEL, A. NYLANDSTED LARSEN, H.H. HANSEN
  Half-life of the 6.21 keV level in ^{181}Ta.
  Z. Phys. A 300, 85 (1981).

- R. VANINBROUKX, G. GROSSE, W. ZEHNER
  New determination of the half-lives of ^{57}Co, ^{103}Rn, ^{103m}Rh, ^{103}Pd and ^{109}Cd.
  Int. J. Appl. Radiat. Isot. 32, 589 (1981).

- R. VANINBROUKX, W. ZEHNER
  Determination of the KX-ray emission probability in the decay of ^{103m}Rh.
  Int. J. Appl. Radiat. Isot., 32, 850 (1981).

- W. BAMBYNEK
  X-ray fluorescence yields, Auger and Coster-Kronig transition probabilities.
  This Week Citation Classics in Current Contents, 21, Nos. 41, 22 (1981).

- A. KACPEREK, B. DENECKE, D. REHER, W. BAMBYNEK
  The standardization of X-ray sources below 4 keV.
  Nucl. Instr. Meth., in press.

- R. VANINBROUKX, B. DENECKE
  Determination of γ-ray emission probabilities in the decay of ^{235}U and ^{231}Th.
  Nucl. Instr. Meth., in press.

- D. REHER, I.V. MITCHELL, W. OLDENHOF
  The preparation and characterization of radioactive sources of refractory metals for low energy X-ray and electron spectrometry.
  Nucl. Instr. Meth., in press.

- D. REHER
  The internal conversion in ^{93m}Nb.
  Int. J. Appl. Radiat. Isot., in press.

- H.H. HANSEN, D. MOUCHEL, A. NYLANSTED LARSEN
  Half-life of the 37.1 keV level in ^{121}Sb.
  submitted to Z. Phys. A.

Conference papers

- B. DENECKE
  Superficial density measurements by electron absorption in air pollution samples.
  Proceedings of the International Conference on Industrial Application of Radioisotopes and Radiation Technology, Grenoble, 28 September - 2 October, 1981, in press.

- G. BORTELS, D. REHER, R. VANINBROUKX
  Emission probability for the 4.45 meV alpha particles in the decay of ^{224}Ra.
  ICRM Seminar on Alpha Spectrometry Techniques and Applications, Geel, 14 October 1981, to be published in Int. J. Appl. Radiat. Isot.

Reports

- G. BORTELS
  Determination of the alpha activity ratio $^{228}Th/^{232}U$ in the Harwell spike solution used in the USIP phase III.
  in: M. Ivanovich and R.M. Warchal (eds.), Report on the Second Uranium-Series Intercomparison Project Workshop, Harwell, 24-25 June 1980, AERE-R 10044 (1981), p. 34.

- H.H. HANSEN
  Compilation of experimental values of internal conversion coefficients and ratios for nuclei with $Z \leqslant 60$.
  Physik Daten/Physic Data 17-1 (1981) (Fachinformationszentrum Energie, Physik, Mathematik, Karlsruhe).

- R. VANINBROUKX
  Status report, JRC-CBNM participation in the IAEA coordinated research programme on the measurement and evaluation of transactinium nuclear decay data.
  in: A. Lorenz (ed.), Fourth coordinated research meeting on the measurement and evaluation of transactinium isotope nuclear data, Vienna, 12-13 October, 1981.
  INDC(NDS)-report, in press.

- W. BAMBYNEK
  Decay data measured at CBNM since 1968.
  in: D.D. Hoppes and F.J. Schima, Nuclear Data for the Efficiency Calibration of Germanium Spectrometer Systems.
  NBS Special Publication, in press.

CINDA ENTRIES LIST

ELEMENT S	A	QUANTITY	TYPE	ELEMENT MIN	MAX	DOCUMENTATION REF	VOL	PAGE	DATE	LAB	COMMENTS
LI	006	N,TRITON	EXPT-PROG	NDG		INDC(EUR)	15	36	382	GEL	BASTIAN+REL TO B10(N,A),TBD
LI	006	N,TRITON	EXPT-PROG	10+1	33+5	INDC(EUR)	15	37	382	GEL	KNITTER+ANGDIST,LEG COEF
LI	007	N,N TRITON	EXPT-PROG	60+6	10+7	INDC(EUR)	15	19	382	GEL	LISKIEN+ANGDIST,LEG COEF,E'DIST
LI	007	N,N TRITON	EXPT-PROG	47+6	80+6	INDC(EUR)	15	19	382	GEL	LISKIEN+ACT METHOD
S	032	N,ALPHA	EXPT-PROG	50+3	40+5	INDC(EUR)	15	33	382	GEL	WAGEMANS+TBD LINAC TOF
S	032	RESON PARAMS	EXPT-PROG	10+5	20+6	INDC(EUR)	15	26	382	GEL	JUNGMANN+ANAL OF TOT + DEL XSECT
K	040	N,ALPHA	EXPT-PROG	20-2	70+4	INDC(EUR)	15	34	382	GEL	WEIGMANN+LINAC TOF
K	040	N,PROTON	EXPT-PROG	20-2	70+4	INDC(EUR)	15	34	382	GEL	WEIGMANN+LINAC TOF
FE		N,ALPHA	EXPT-PROG	14+7		INDC(EUR)	15	20	382	GEL	WATTECAMPS+TBD
FE	054	N,GAMMA	EXPT-PROG	70+3	30+5	INDC(EUR)	15	13	382	GEL	ALLEN+LINAC TOF
FE	054	RESON PARAMS	EXPT-PROG	70+3	30+5	INDC(EUR)	15	13	382	GEL	ALLEN+LINAC TOF
CR		N,ALPHA	EXPT-PROG	14+7		INDC(EUR)	15	20	382	GEL	WATTECAMPS+TBD
NI		N,ALPHA	EXPT-PROG	14+7		INDC(EUR)	15	20	382	GEL	WATTECAMPS+TBD
CU	063	N,ALPHA	EXPT-PROG	NDG		INDC(EUR)	15	39	382	GEL	LISKIEN+REL TO AL(N,A),AVER XSECT
SR	088	RESON PARAMS	EXPT-PROG	NDG		INDC(EUR)	15	34	382	GEL	ALLEN+LINAC TOF CAPT YIELD
ZR	096	N,GAMMA	EXPT-PROG	17+2	90+4	INDC(EUR)	15	15	382	GEL	ALLEN+LINAC TOF
ZR	096	RESON PARAMS	EXPT-PROG	30+2	30+4	INDC(EUR)	15	15	382	GEL	ALLEN+LINAC TOF
PD	104	N,GAMMA	EXPT-PROG	50+0	60+5	INDC(EUR)	15	18	382	GEL	BASTIAN+AVERAGE XSECT
PD	104	RESON PARAMS	EXPT-PROG	10+0	20+4	INDC(EUR)	15	16	382	GEL	STAVELOZ+
PD	105	N,GAMMA	EXPT-PROG	25-2		INDC(EUR)	15	18	382	GEL	BUYL+
PD	105	N,GAMMA	EXPT-PROG	50+0	60+5	INDC(EUR)	15	18	382	GEL	BASTIAN+AVERAGE XSECT
PD	105	RESON PARAMS	EXPT-PROG	10+0	20+3	INDC(EUR)	15	16	382	GEL	STAVELOZ+
PD	106	N,GAMMA	EXPT-PROG	50+0	60+5	INDC(EUR)	15	18	382	GEL	BASTIAN+AVERAGE XSECT
PD	106	RESON PARAMS	EXPT-PROG	10+0	20+4	INDC(EUR)	15	16	382	GEL	STAVELOZ+
PD	108	N,GAMMA	EXPT-PROG	25-2		INDC(EUR)	15	18	382	GEL	BUYL+
PD	108	N,GAMMA	EXPT-PROG	50+0	60+5	INDC(EUR)	15	18	382	GEL	BASTIAN+AVERAGE XSECT
PD	108	RESON PARAMS	EXPT-PROG	10+0	20+4	INDC(EUR)	15	16	382	GEL	STAVELOZ+
PD	110	N,GAMMA	EXPT-PROG	50+0	60+5	INDC(EUR)	15	18	382	GEL	BASTIAN+AVERAGE XSECT
PD	110	RESON PARAMS	EXPT-PROG	10+0	20+4	INDC(EUR)	15	16	382	GEL	STAVELOZ+
TH	232	FRAG SPECTRA	EXPT-PROG	15+6	18+6	INDC(EUR)	15	41	382	GEL	BUDTZ-JORGENSEN+ANGDIST+E'DIST
U	233	N,FISSION	EXPT-PROG	10-2	10+5	INDC(EUR)	15	3	382	GEL	WAGEMANS+REL TO B10(N,A)
U	235	N,FISSION	EXPT-PROG	20+3	85+4	INDC(EUR)	15	5	382	GEL	CORVI+AVERAGE VALUES
U	235	N,GAMMA	EXPT-PROG	20+3	85+4	INDC(EUR)	15	5	382	GEL	CORVI+AVERAGE VALUES
U	235	ALPHA	EXPT-PROG	20+3	85+4	INDC(EUR)	15	5	382	GEL	CORVI+AVERAGE VALUES
U	235	ALPHA	EXPT-PROG	60+0	14+2	INDC(EUR)	15	7	382	GEL	CORVI+AVERAGE VALUES
U	235	FRAG SPECTRA	EXPT-PROG	NDG		INDC(EUR)	15	4	382	GEL	ALLAERT+DEPEND ON RESON SPIN
U	235	FRAG SPECTRA	EXPT-PROG	15+5	10+7	INDC(EUR)	15	41	382	GEL	BUDTZ-JORGENSEN+ANGDIST+E'DIST
PU	238	N,FISSION	EXPT-PROG	15+5	10+7	INDC(EUR)	15	8	382	GEL	KNITTER+REL U235(N,F)
PU	238	N,FISSION	EXPT-PROG	10+1	10+6	INDC(EUR)	15	8	382	GEL	KNITTER+LINAC TOF REL LI6(N,A)
PU	240	N,FISSION	REVW-PROG	NDG		INDC(EUR)	15	42	382	GEL	KNITTER+SEC CHANCE FISS THRESH
PU	240	RESON PARAMS	REVW-PROG	NDG		INDC(EUR)	15	9	382	GEL	WEIGMANN
PU	241	N,FISSION	EXPT-PROG	10-2	30+4	INDC(EUR)	15	3	382	GEL	WAGEMANS+REL TO B10(N,A)
PU	241	FRAG SPECTRA	EXPT-PROG	NDG		INDC(EUR)	15	4	382	GEL	ALLAERT+DEPEND ON RESON SPIN
PU	241	FRAG SPECTRA	EXPT-PROG	25-2		INDC(EUR)	15	4	382	GEL	ALLAERT+
PU	242	N,FISSION	EXPT-PROG	10+2	20+3	INDC(EUR)	15	10	382	GEL	WARTENA+LINAC TOF
PU	242	N,FISSION	REVW-PROG	NDG		INDC(EUR)	15	42	382	GEL	KNITTER+SEC CHANCE FISS THRESH
PU	242	RESON PARAMS	REVW-PROG	NDG		INDC(EUR)	15	9	382	GEL	WEIGMANN
PU	242	FRAG SPECTRA	EXPT-PROG	SPON		INDC(EUR)	15	4	382	GEL	ALLAERT+
PU	244	N,FISSION	EXPT-PROG	10+3	50+6	INDC(EUR)	15	10	382	GEL	MOORE+
PU	244	N,FISSION	REVW-PROG	NDG		INDC(EUR)	15	42	382	GEL	KNITTER+SEC CHANCE FISS THRESH
AM	241	N,GAMMA	EXPT-PROG	NDG		INDC(EUR)	15	11	382	GEL	CORNELIS+LINAC TOF

Edited by G.H. DEBUS